Ann. Rev. Astron. Astrophys. 1986. 24 : 459–97

GLOBAL STRUCTURE OF MAGNETIC FIELDS IN SPIRAL GALAXIES

Yoshiaki Sofue

Nobeyama Radio Observatory and Department of Astronomy, University of Tokyo, Minamisaku, 384-13 Nagano, Japan

Mitsuaki Fujimoto

Department of Astrophysics, Nagoya University, Chikusa, 464 Nagoya, Japan

Richard Wielebinski

Max-Planck-Institut für Radioastronomie, Auf dem Hügel 69, D-5300 Bonn 1, West Germany

1. INTRODUCTION

The configuration of magnetic fields in spiral galaxies is intimately related to the magnetohydrodynamic behavior of interstellar gases and is closely linked to the formation of gaseous arms and magnetoionic halos surrounding the galactic disks. In spite of the clear evidence for nonthermal emission in spiral galaxies (e.g. Pooley 1969, Mathewson et al. 1972, van der Kruit & Allen 1976, Wielebinski 1985), which indicates the existence of magnetic fields, the physics of the formation of spiral arms have been discussed in the last few decades mainly on the basis of the gravitational and gas-dynamical treatment of matter, e.g. the density-wave theory (Lin et al. 1968, Lin 1971) and the galactic shock-wave theory (Fujimoto 1966, Roberts 1969, 1975, Roberts & Yuan 1970). This "pan-gravitationalism" trend of understanding the spiral structure may have resulted from the

0066–4146/86/0915–0459$02.00

lack of observational data of the large-scale configuration of magnetic fields; such data are essential in treating the relation of the gas to the magnetic field. Recent observations of magnetic fields in galaxies (Segalovitz et al. 1976, Tosa & Fugimoto 1978, Beck et al. 1980, Klein et al. 1982, 1983a, van Albada & van der Hulst 1982, Sofue et al. 1985) have provided clear evidence of the large-scale alignment of the fields in nearby galaxies. These fields must be taken into account for a full magnetohydrodynamical treatment of the spiral arms.

In contrast to the situation in external galaxies, the local magnetic field in our Galaxy has been extensively studied in the past few decades, and the galactic magnetic field has been reviewed in several articles (e.g. Gardner & Whiteoak 1966, Heiles 1976, Spoelstra 1977, Manchester & Taylor 1977, Verschuur 1979, King 1983, Vallée 1984).

The origin of magnetic fields in disk galaxies has been interpreted from two controversial points of view. On the one hand, we have the dynamo theory (Parker 1971a,b, 1979, Stix 1975, 1976), which requires a circular magnetic field configuration. Another hypothesis postulates the primordial origin of the field (e.g. Piddington 1964, 1972, 1978, Ohki et al. 1964) and predicts a bisymmetric spiral configuration open to the intergalactic space. To resolve the question of which of these alternative theories does apply, efforts have been made to map magnetic fields in nearby galaxies. The observational data have now reached a stage where serious discussion of the different interpretations can be made.

In this review we survey the observational techniques, the current observational data, and the methods used to derive the field configurations in spiral galaxies. We also discuss the field configurations and their implications on the dynamics, evolution, and activity in spiral galaxies.

2. MEASUREMENT TECHNIQUES

The basic information about the presence and structure of magnetic fields in galaxies is obtained from optical and radio observations. The optical polarization observations show the presence of magnetic fields that align the dust grains. These grains are apparently elongated and scatter light preferentially in one plane. Polarized radio emission originates in the synchrotron process. The plane of the polarization is determined by the direction of the magnetic field. The intensity of the radio emission depends on the magnetic field strength. The latter fact allows us, upon the assumption of equipartition, to determine the field strength. The polarized wave suffers a Faraday rotation in the interstellar plasma. A product of longitudinal field strength, thermal electron density, and path length can be deduced from Faraday rotation measures. A direct magnetic field measure-

ment can be made using the Zeeman effect. In addition, circular polarization is a direct probe of the magnetic field strength. In the following sections, the various techniques are discussed in more detail.

2.1 *Optical Polarization*

The first evidence for interstellar magnetic fields comes from measurements of optical polarization. The first results for an external galaxy were reported by Öhman (1942) for M31. The basic mechanism (so-called Davis-Greenstein effect) that is responsible for the optical polarization is the scattering of light by elongated dust grains aligned by the magnetic fields (Davis & Greenstein 1951, Purcell & Spitzer 1971, Spitzer 1978, Savage & Mathis 1979). We can measure the linear polarization of stars or of globular clusters in the nearest galaxies. Polarimetric techniques can also be used (e.g. Scarrott et al. 1977), which enable a whole galaxy to be surveyed. Optical polarization measurements, however, give no field strength, only the orientation of the field. The field alignment is expected to be such that the optical E vector is parallel to the field orientation.

The usual interpretation of the optical polarization from galaxies is that we are observing starlight transmitted through dust grains aligned by a magnetic field. However, the effect of diffuse scattered light by dust is probably also causing the polarization and must be mixed with a considerable amount of direct starlight (Elvius 1978a,b, Jura 1979, 1982). Further observational tests using infrared polarization may be necessary to clarify this question (Jura 1982).

2.2 *Radio Polarization*

The synchrotron emission is in general elliptically polarized (e.g. Ginzburg & Syrovatskii 1965, 1969, Gleesen et al. 1974, Gardner & Whiteoak 1966, Moffet 1973, Pacholczyk 1976). The electric (E) vector of the linear component (which can be up to $P_{\max} = (\gamma+1)/(\gamma+7/3) \approx 70$–$75\%$, with γ the power spectral index of emitting electrons) is perpendicular (transverse) to the orientation of the magnetic field. In some parts of the Galaxy, in nearby galaxies, and in radio galaxies, linear polarization of up to 70% has been detected, indicating a high degree of field alignment. Linearly polarized radio waves are subject to Faraday rotation during the transition of a magnetoionic plasma. The Faraday effect can be used in turn to determine the longitudinal magnetic field if path length and thermal electron density are known. Finally, we can determine the magnetic field strength by the use of the arguments of equipartition between the energy in the magnetic field and the cosmic rays. All these uses of radio polarization data for the determination of magnetic fields (or products of various parameters) are discussed in the following sections in more detail.

FIELD COMPONENT TRANSVERSE TO THE LINE OF SIGHT The direction of the line of force projected on the sky, or the field component perpendicular to the line of sight, can be obtained by radio measurements. The orientation of the "E" vector in the emitting region is perpendicular to the magnetic field (Ginzburg & Syrovatskii 1965). The emission that leaves the emitting region perpendicular to (an aligned) magnetic field suffers no Faraday rotation. However, in general the observed position angle ϕ of the linearly polarized emission is given by

$$\phi = \phi_0 + \phi_F, \tag{2.1}$$

where ϕ_0 is the intrinsic position angle and ϕ_F is the additional Faraday rotation. Note that the Faraday rotation is a summation of effects in all the components of the magnetoionic medium between the emission region and the observer.

The Faraday rotation is given by (Gardner & Whiteoak 1966, Burn 1966)

$$\phi_F = RM\lambda^2 \text{ [rad]}, \tag{2.2}$$

where RM is the rotation measure in rad m^{-2}, and λ is the wavelength in meters; furthermore, we have

$$RM = 0.81 \int n_e B_\parallel dl, \tag{2.3}$$

where n_e is the thermal electron density in cm^{-3}, $B_\parallel$ is the parallel (longitudinal) field in μG, and l is the path length in pc.

Thus, to derive the intrinsic position angle it is necessary, by measurement at a number of wavelengths, to correct for the Faraday rotation. Alternatively, observations should be made at such a high radio frequency so that we measure the intrinsic position angle ϕ_0.

FIELD COMPONENT PARALLEL TO THE LINE OF SIGHT The Faraday effect makes possible the determination of the longitudinal component of the magnetic field. By measuring the position angle ϕ at several wavelengths, we can determine both ϕ_0 and RM at the same time. The position angle ϕ_B of the magnetic field projected on the sky is given by

$$\phi_B = \phi_0 + \frac{\pi}{2}. \tag{2.4}$$

Only through observations at a number of frequencies (at least three) can the ambiguity of $n\pi$ in angle be eliminated.

One of the problematical aspects of Faraday rotation is the fact that it

occurs along the whole path between the emitting source and the observer. In fact, the RM is the summation of the various components

$$RM = RM_g + RM_{IG} + RM_G, \quad 2.5$$

where RM_g is the component occurring in a galaxy, RM_{IG} is that between the galaxy and the Galaxy, and RM_G is due to the Galaxy.

The RM_G component has been studied by observations of polarized extragalactic sources. It must be comparable to RM_g. However, the angular scale size of variation of RM_g over a galaxy is much smaller compared with that of RM_G in the Galaxy. Thus RM_G can be regarded as a "DC" component in Equation 2.5 when discussing an internal variation of RM_g of a galaxy, which is the main topic of interest in this article. The intergalactic contribution is small, certainly $|RM_G| \lesssim 1$ rad m^{-2} (Kronberg & Simard-Normandin 1976, Sofue et al. 1979, Weller et al. 1984).

The thermal electron density n_e in the Galaxy has been approximated in a number of ways, but it is not well known. The best value comes from the study of the dispersion measure toward pulsars (e.g. Manchester & Taylor 1977). The mean electron density value of $\overline{n_e} \sim 0.03$ cm^{-3} is certainly the best present characterization of the results. However, variations between $0.1 > \overline{n_e} > 0.01$ are known. The local thermal electron densities (for example, in a molecular cloud) could be greater by an order of magnitude.

MAGNETIC FIELD STRENGTH FROM EQUIPARTITION The most common way to determine the strength of the magnetic field is to assume the equipartition between the energy density of cosmic rays and the magnetic field. We assume an ensemble of relativistic electrons having an energy spectrum of the form

$$N(E)\,dE = N_0 E^{-\gamma}\,dE. \quad 2.6$$

For the equipartition, we then have

$$\frac{B^2}{8\pi} = a\int_{E_1}^{E_2} EN(E)\,dE, \quad 2.7$$

where E_1 and E_2 are the lower and upper limits to the energy spectrum and correspond to the lower and upper cutoff frequencies ν_1 and ν_2 of the synchrotron radio spectrum, respectively. Here, a is the ratio of the total energy of cosmic rays to the electron energy. The field strength B (in G) is then given by (Moffet 1973)

$$B = 2.3(aA\varepsilon)^{2/7}, \quad 2.8$$

where ε is the volume emissivity (in erg s^{-1} cm^{-3}), and A is given by

$$A = C\left(\frac{\alpha+1}{\alpha+1/2}\right)\left(\frac{\nu_2^{\alpha+1/2}-\nu_1^{\alpha+1/2}}{\nu_2^{\alpha+1}-\nu_1^{\alpha+1}}\right). \quad 2.9$$

Here C is a constant of 1.057×10^{12} in cgs units, and α $[=-(\gamma-1)/2]$ is the radio spectral index. The emissivity is given by

$$\varepsilon = \frac{4\pi}{l}\int_{\nu_1}^{\nu_2} I_\nu \, d\nu, \quad 2.10$$

where I_ν is the intensity and l (cm) is the path length of the source. The parameters a and ν_1 (Hz) are often taken as 100 and 10^7, respectively (Moffet 1973). However, Beck (1983) used a somewhat more sophisticated method to determine the coefficient a from an empirical relationship between the radio intensity of our Galaxy and its magnetic field strength in the solar neighborhood.

The basic premise of equipartition is open to discussion. However, the results for external galaxies seem to be in reasonable agreement with values found in our own Galaxy by other methods. Also, these arguments do not prejudice our comparison of different objects.

The nonthermal (synchrotron) component can be separated from the thermal component by studying a galaxy at several frequencies (e.g. Klein & Emerson 1981, Gioia et al. 1982).

The linear polarization degree p of the radio emission is used to determine the ratio of uniform component B_u to total strength of the field B_t ($f = B_u/B_t$) by employing the formula given by Segalovitz et al. (1976). The random component B_r can be calculated through $B_t^2 = B_u^2 + B_r^2$. Normal spiral galaxies have a value of about $B_u/B_r \approx 0.5$.

OTHER POSSIBLE OBSERVING TECHNIQUES The Zeeman effect [splitting of the H I (or OH) line in a magnetic field] has been observed (e.g. Verschuur 1974, 1979) in dense interstellar clouds in the Galaxy. There have been no reports of this type of observation in an external galaxy.

In strong aligned magnetic fields or in the case of mildly relativistic electrons, circular polarization is emitted (e.g. Legg & Westfold 1968). Circular polarization suffers no Faraday rotation and could be a useful method of probing the magnetic fields. Circular polarization has been observed in solar flares, the planet Jupiter, and pulsars. Certainly the fields in these objects are $1–10^{12}$ G, far stronger than those in interstellar space. In other sources (e.g. quasars) the circular component is less than 0.5%. So far, no results are available for external galaxies.

FARADAY ANALYSIS OF A GALAXY The positional variation of the RM_g component in Equation 2.5 over a galaxy is used to study the configuration of a global magnetic field under the assumption that the field is distributed in the plane of the galaxy. The method proposed by Tosa & Fujimoto (1978) assumes two predominant configurations of the field in galaxies (Figure 1). One is the circularly oriented field configuration concentric to the galaxy center, or a ring field. The other is a configuration with a bisymmetric spiral (BSS) magnetic field in which the lines of force run into the disk from one side of the galaxy plane and go out from the diametrically opposite side into intergalactic space. Higher order and/or random components must be superimposed on the large-scale field. However, such smaller scale structures have been smeared out by the finite beam width, except for the local field in our Galaxy.

"RM-θ" method Suppose that the field has a ring configuration confined within an inclined thin disk. Then the line-of-sight field direction at a point on the major axis is opposite to that at the diametrically symmetric point. The line-of-sight field component changes sinusoidally as a function of the azimuthal angle θ along a circle concentric to the center. Thus the rotation measure varies as

$$RM_g = RM_0 \cos\theta \tan i \qquad 2.11$$

with i the inclination of the galaxy (edge-on for $i = 90°$). The "characteristic rotation measure" RM_0 is defined through

$$RM_0 = 0.81 \int_0^\infty n_e(z) B_0(z)\, dz \quad (\text{rad m}^{-2}). \qquad 2.12$$

Here $B_0(z)$ (μG) is the absolute field strength of the ordered component along the circle as a function of the distance z (pc) from the galactic plane, and $n_e(z)$ is the electron number density (cm^{-3}), again as a function of z.

If the field configuration is bisymmetric spiral, the rotation measure varies with θ in the following way (Tosa & Fujimoto 1978, Sofue et al. 1980):

$$\begin{aligned} RM_g &= RM_0 \cos(\theta - p) \cos(\theta - m) \tan i, \\ &= \frac{1}{2} RM_0 \tan i\, [\cos(2\theta - p - m) + \cos(p - m)], \end{aligned} \qquad 2.13$$

where p is the pitch angle of the spiral field direction and m the position angle at the maximum field strength on the circle. Figure 1 illustrates

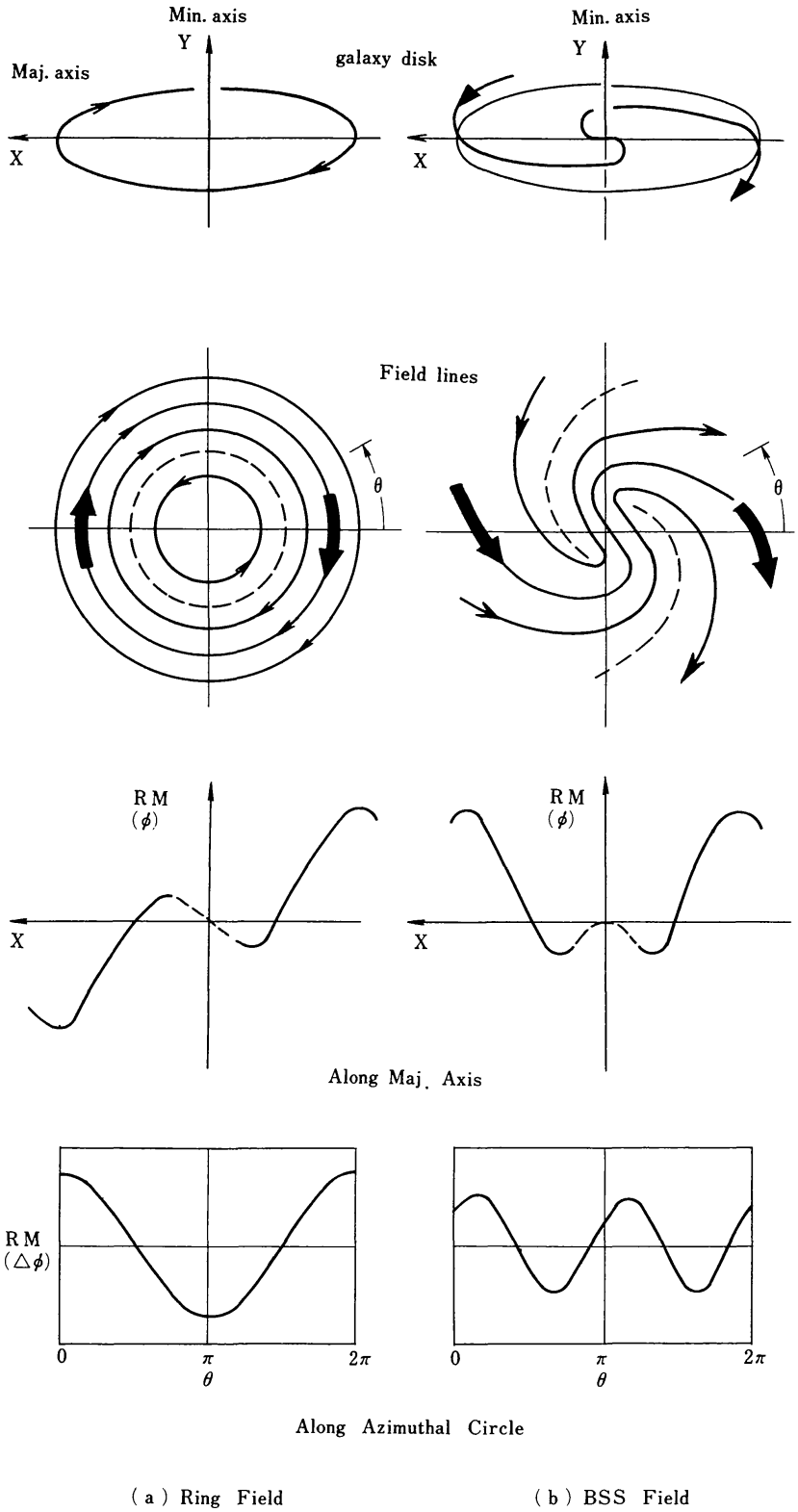

Figure 1 The ring and bisymmetric (BSS) magnetic field configurations in disk galaxies. The characteristic variations of RM, ϕ, or $\Delta\phi$ are illustrated against the distance along the major axis and against the azimuthal angle θ along a circle.

the bisymmetric spiral field configuration and the variation of RM_g as a function of θ.

The essential difference between Equations 2.11 and 2.13 is that the rotation measure varies with the azimuthal angle θ in a single-sinusoidal way for a ring field, whereas it varies in a double-sinusoidal way for a BSS field (Figure 1).

"$\Delta\phi$-θ" method As is readily shown, the polarization angle at a certain frequency varies with θ as

$$\phi = \lambda^2 RM_g(\theta) + \phi_0 + \phi_{IG+G}, \qquad 2.14$$

where $\phi_0 = \phi_B - 90°$ is the intrinsic polarization angle (usually taken perpendicular to the spiral arm with a fixed pitch angle or to the azimuthal ring), and ϕ_{IG+G} is the foreground rotation, which is assumed to be constant over a galaxy. Equation 2.14 allows us to determine RM_g, and so RM_0; furthermore, we can use it to distinguish the field configuration from a single-frequency observation by plotting $\Delta\phi = \phi - \phi_0$ against the azimuthal angle θ, where $\phi - \phi_0$ is the angle between the observed polarization plane and the intrinsic polarization plane, which is locally perpendicular to the spiral arms. This method may be referred to as the "$\Delta\phi - \theta$" method (Sofue et al. 1980).

"ϕ-x" method A simpler method of discriminating between the ring and bisymmetric field configurations has been proposed by Sofue et al. (1985). If the field configuration is a ring (Figure 1), then RM_g, and therefore the observed polarization angle ϕ, varies along the major axis antisymmetrically with respect to the galaxy center, and thus no variation should be observed along the minor axis. On the other hand, if the field is bisymmetric spiral, the variations along both the major and minor axes are symmetric with respect to the galaxy center (Figure 1). This method applies for polarization scans along only the major and minor axes, and therefore deeper and more sensitive observations are possible within a limited observing time. With this method we can increase the number of sample galaxies rather easily. The method is referred to hereafter as the "ϕ-x" method, where x is the distance along the major axis of the galaxy center.

3. GLOBAL MAGNETIC FIELDS IN SPIRAL GALAXIES

3.1 *Optically Determined Fields*

Magnetic field structures for the Milky Way Galaxy as derived from starlight polarization have been described in several articles (Aannestad &

Purcell 1973, Heiles 1976, Mathewson & Ford 1970b, Ellis & Axon 1978). However, these observations reveal only a local field structure within a few kiloparsecs of the Sun.

The predominant magnetic field in normal spiral galaxies as derived from optical observations seems to be parallel to the spiral arms in the first approximation (see Table 1). However, some claim has been made of the plausibility of interpreting the polarization as resulting from the magnetic field origin (see Section 2.2). Given the present-day accuracy of optical observations, however, it is difficult to say whether the field is ring-like or a spiral having some pitch angle to the azimuthal circle.

SPIRAL GALAXIES Starlight polarization has been observed for a fair number of galaxies, most of which are spirals (Elvius 1969, 1972, 1978a,b, Levy 1978). The spirals NGC 4216, NGC 3623, and NGC 5055 are known to possess large-scale magnetic fields aligned parallel to the spiral arms from the fact that their polarization vectors are predominantly parallel to their spiral arm direction when projected onto the sky. Edge-on galaxies are shown to possess starlight polarization parallel to their dark lanes, which suggests that the magnetic fields in these galaxies are also parallel to the spiral arms. Examples are seen in NGC 4565 (Elvius 1972), NGC 7814, NGC 5128 (Cen A: a dark lane along the minor axis of the elliptical galaxy; Elvius & Hall 1964), and NGC 4590 (M104: Sombrero galaxy; Appenzeller 1967, Scarrott et al. 1977).

Table 1 Optically determined magnetic fields in galaxies[a]

Galaxy	Field direction	Remarks
NGC 224	Parallel to arms	M31, globular clusters
NGC 3190	Parallel to dark lane	
NGC 3623	Parallel to arm	Contaminated by scattered light
NGC 3718	Not parallel to arms	Peculiar
NGC 4216	Parallel to arm	Contaminated by scattered light
NGC 4565	Parallel to dark lane	Edge on
NGC 4590	Parallel to dark lane	M104 (Sombrero), scattered light in halo
NGC 5055	Parallel to arm	
NGC 5128	Parallel to dark lane	Cen A: a dark lane perpendicular to the ellipsoid
NGC 5283	Parallel to dark lane	SB galaxy
NGC 7814	Parallel to dark lane	Edge on
LMC/SMC	Parallel to line LMC-SMC?	Magnetic envelope?

[a] See text for references. Optical polarization measurements have been made of some other galaxies such as NGC 3034 (M82), NGC 2685, and NGC 7331, but their polarization is believed to result from scattered light (see text).

The effect of scattering is probably also causing the polarization of light, with the electric vector parallel to the symmetry axis of the brighter side of spiral galaxies like NGC 3623, NGC 4216, and NGC 7331. The polarized scattered light must be mixed with a considerable amount of direct starlight (Elvius 1978a). Jura (1979, 1982) has claimed that the starlight polarization observed for NGC 5128 and NGC 4590 might be due to such a scattering effect, and that the starlight polarization observed for the inner region of M31 and M81 might also result from scattering of grains.

In the case of M31, the nearest spiral galaxy, individual globular clusters have been studied (Hiltner 1958, Martin & Shawl 1979, 1982); these clusters reveal polarization vectors consistent with a circular magnetic field. In this case, the starlight is more directly transmitted through the disk, and the polarization is clearly due to dust grains in the galactic disk aligned by the magnetic field.

IRREGULAR AND PECULIAR GALAXIES M82 (NGC 3034) has been well studied in optical polarization, in which the scattered light is the major source of the observed polarization pattern (Solinger 1967, Solinger & Markert 1975, Schmidt et al. 1976, Visvananthan 1974, Bingham et al. 1976). The electric vectors are distributed concentric to the galaxy center, and the polarization is as large as 10% in the space high above the galactic plane by 1–2 kpc. The polarization is well interpreted as resulting from scattering of strong starlight from the nuclear region by dust grains distributed in the halo. In fact, it is well known that M82 has dusty lanes running into its halo high above the galactic disk (Lynds & Sandage 1963).

NGC 3718 and NGC 2685 are examples of peculiar galaxies where the polarization effects have been observed to indicate large-scale magnetic fields connected with structures other than ordinary spiral arms (Elvius 1978a). The bright parts of arc-like filaments in NGC 2685 may, however, show effects of starlight scattering similar to those for M82.

Polarization toward the Large Magellanic Cloud was reported to suggest the existence of a large-scale magnetic field running along the main "bar" in the Cloud (by N. Visvananthan: cited in Bok 1966). Polarization of bright stars in the Magellanic Clouds was observed by Mathewson & Ford (1970) and Schmidt (1970, 1976). They have shown also that there exist largely aligned magnetic fields in the Clouds.

3.2 *Field Configurations Derived From Radio Observations*

Quantitative and three-dimensional field structures can be studied by radio observations. The observational facts with regard to the large-scale magnetic fields in the disks of spiral galaxies so far known from Faraday

rotation analyses may be summarized as follows: *The predominant configuration of the large-scale field in a spiral galaxy is either bisymmetric spiral (BSS), with the lines of force possibly open to intergalactic space, or a ring with closed circular field lines in the disk.*

The majority of the spirals are shown to possess a BSS field, whereas only a minority such as M31 have a ring configuration. Table 2 summarizes the derived configurations for the spiral galaxies studied so far, together with their field strength. Structures of order higher than the ring or BSS configuration are also expected to exist in these galaxies. But the observational accuracy is still too poor to reveal finer structures, except for the well-studied local field in our Galaxy. In what follows, we describe some individual galaxies for which the field configurations have been fairly well determined (mainly by the Faraday analyses).

M31 (NGC 224) The first definite map of the linear polarization of M31 was presented by Beck et al. (1980) at 11-cm wavelength. They suggested an orientation of the magnetic field along the bright radio ring at a galactocentric distance $R = 10$ kpc. Sofue & Takano (1981) and Beck (1982) have applied the Faraday analysis described in Section 2.2 and have shown that the Faraday rotation angle $\Delta\phi$ varies with the azimuthal angle θ in a single-sinusoidal way ($\Delta\phi$-θ plot; see Figure 2) for a wide range of galactocentric distances.

The maximum and minimum rotation measures appear on the major axis at the azimuthal angles $\theta = 0°$ and 180°, respectively, which indicates

Table 2 Magnetic fields in galaxies derived from radio observations[a]

Galaxy	Type	Field configuration	Method	Field strength (μG)	Remarks
The Galaxy	Sb	BSS	$RM(l, b)$	$3 \sim 4$	
M31 (NGC 224)	Sb	Ring	$\Delta\phi$-θ	$3 \sim 4$	
M33 (NGC 598)	Scd	BSS	$RM/\Delta\phi$-θ	3 ± 1	
M51 (NGC 5194)	Sc	BSS	RM-θ	10	
M81 (NGC 3031)	Sb	BSS	$\Delta\phi$-θ	8 ± 3	
M83 (NGC 5236)	SBc	BSS	$\Delta\phi$-θ/ϕ-X	—	
NGC 253	Sc(p)	BSS?	ϕ-X	10	
IC 342	Scd	Ring	ϕ-X	7 ± 2	
NGC 6946	Scd	BSS	$\Delta\phi$-θ	12 ± 4	
NGC 2903	Sbc	BSS	ϕ-X	—	
NGC 5055 (M63)	Sc	BSS?	ϕ-X	—	
NGC 4258	SBc	—	—	—	B along anomalous arms
SMC	Irr	—	—	—	Polarized E vectors are perpendicular to the major axis

[a] For references, see the text. The field strength was mainly taken from Beck (1983).

a circularly oriented magnetic field. The amplitude of *RM* variation is about 90 rad m^{-2} ($=RM_0 \tan i$), which yields the characteristic *RM* of $RM_0 = 26$ rad m^{-2} and leads to a mean field strength of the uniform component along the ring as 2–3 μG, where the mean electron density is taken as 0.03 cm^{-3} and the effective thickness of the disk as 500 pc. The characteristic RM_0 has the largest value at $R = 10$ kpc and slightly decreases toward both the outer and inner sides from this "10-kpc ring." The total field strength has been determined as being about 4 ± 1 μG from the nonthermal intensity at 11 cm under the assumption of equipartition (Beck 1982). Therefore a considerable fraction of the field (50–60%) is uniformly oriented along the ring. It should also be stressed that no reversal of field direction is found on the scale greater than the angular resolution of the observations (800 pc), and that the field direction is uniform over a wide interval of galactocentric distances ranging from $R \approx 7$ to 14 kpc.

M33 (NGC 598) Polarization data at wavelengths 21 and 11 cm from Beck (1979) were analyzed by Sofue & Takano (1981), who suggested an open spiral field configuration not closed in the disk (Figure 3). The field may be in a configuration open to intergalactic space, in conflict with the dynamo theory for the ring field. However, the variation of *RM* against the azimuthal angle produced results of large ambiguity, and it was difficult to discriminate whether or not the field configuration was BSS. Buczilowski (1985) carried out an extensive survey of linear polarization at 17.4- and 6.3-cm wavelengths. He has combined the existing data of radio polari-

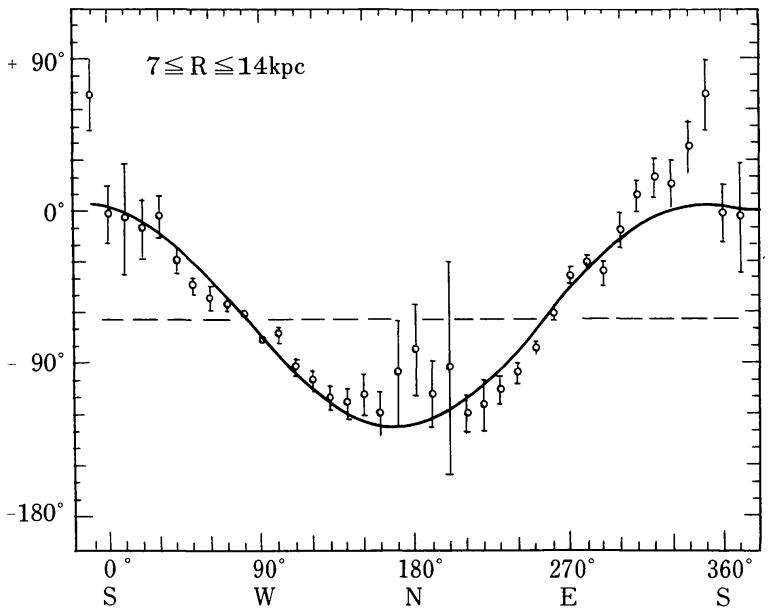

Figure 2 The case of the ring field in M31 (Beck 1982). The single periodic distribution is found in the $\Delta\phi$ distribution against the azimuthal angle θ along a circle at $R = 7$–14 kpc.

zation with his own data, with the result being an unambiguous map of rotation measures. The RM-θ plot indicates a clear BSS characteristic. The measurements show further that the field is well ordered in the northern half of the galaxy, whereas the field alignment and polarization degree are low in the radio-brightest region in the southern half. The latter result may be due to strong interstellar turbulence enhanced by active star formation in the southern half of the galaxy.

M51 (NGC 5194) Mathewson et al. (1972) have mapped this nearly face-on galaxy in radio continuum at 20 cm and have shown that the synchrotron emission comes predominantly from dark lanes along the spiral arms. This fact showed that the galactic shock-wave theory (Fujimoto 1966, Roberts 1969) applies to the formation of the radio arms through a strong compression of gas and magnetic fields with cosmic rays. Segalovitz (1976) and Segalovitz et al. (1976) have mapped linearly polarized emission and have given electric-vector distributions at 1.4 and 5 GHz. Their data show a significant Faraday rotation in the galaxy. Tosa & Fujimoto (1978) analyzed the 1.4- and 5-GHz data and derived both the doubly periodic

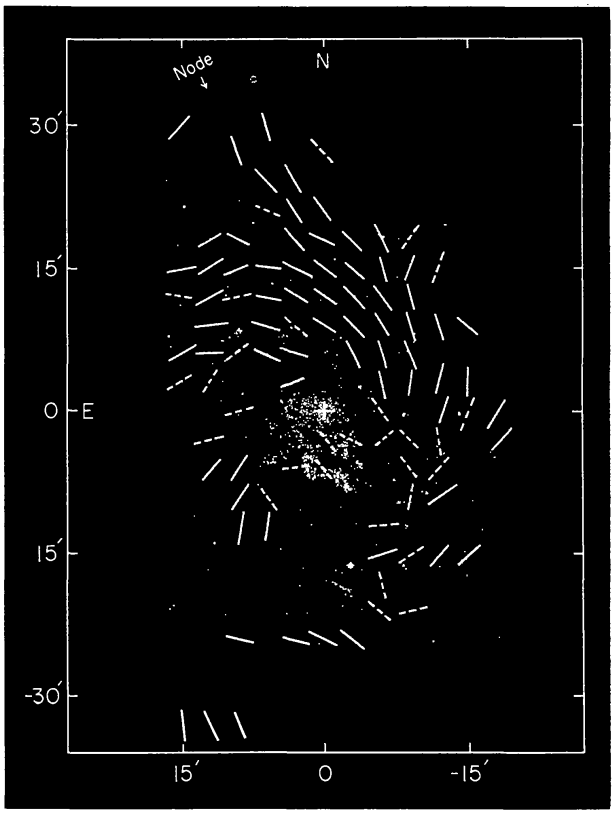

Figure 3 Magnetic field direction in M33 superimposed on a photograph [Sofue & Takano 1981; photo © by the Carnegie Institution of Washington (Sandage 1961)].

distribution of the Faraday rotation angle $\Delta\phi$ against the azimuthal angle θ and the magnetic field component projected onto the sky (Figure 4). Their results concluded that the global magnetic field has a bisymmetric spiral configuration running along the arms (Figure 4) and possibly open to intergalactic space. Sofue et al. (1980) further used the 6-cm data of Segalovitz (1976) to show that the $\Delta\phi$-θ plot has a double-peaked sinusoidal variation and that the corresponding characteristic RM_0 is 60 rad m^{-2}, a value consistent with a BSS configuration of the field.

M81 (NGC 3031) Faraday rotation analysis was applied by Sofue et al. (1980) to the 21-cm polarization data of Segalovitz (1976). They found a doubly sinusoidal variation for the $\Delta\phi$-θ plot and suggested a bisymmetric open spiral configuration of the field. Recent Faraday analysis of the rotation angle at 6.3 cm by Beck et al. (1985) showed also a double-peaked sinusoidal variation on the $\Delta\phi$-θ plot, which again suggested a bisymmetric spiral configuration. However, from the inconsistency of the amplitudes of the rotation (80° and 60° at 21 cm and 6 cm, respectively) for a Faraday effect, Beck et al. (1985) suggested that the observed variation might be due rather to some intrinsic deviation of the field direction from a regular spiral.

Figure 4 Magnetic field direction in M51 superimposed on a photograph [Tosa & Fujimoto 1978; photo © by the Carnegie Institution of Washington (Sandage 1961)].

A polarization degree as high as ~60% detected near the minor axis indicates that the field is highly ordered, running parallel to the spiral arms (Beck et al. 1985). A strong shock compression may be a vital origin for such a highly ordered field. The lower polarization near the major axis shows a significant depolarization due to a large Faraday rotation by the field running nearly tangentially there.

The average total field strength in M81 has been estimated as $B = 8 \pm 3$ μG, about twice as strong as in M31 (Beck 1982) but weaker than in M51 (Klein et al. 1984) or in NGC 6946 (Klein et al. 1982). The average degree of polarization, $p = 14\%$, leads to the uniform and random field strength values of $B_u = 3.0 \pm 1.5$ μG and $B_r = 6.8 \pm 1.5$ μG, respectively (Beck et al. 1985).

NGC 6946 The Scd galaxy NGC 6946 is an almost face-on bright spiral that has a high radio surface brightness. Because of its low galactic latitude ($b = 12°$), optical polarization data are rather poor despite the high optical brightness of the galaxy. Klein et al. (1982) have studied the distribution and polarization at 2.8 cm of this galaxy and have proposed a distribution of magnetic field direction (Figure 5).

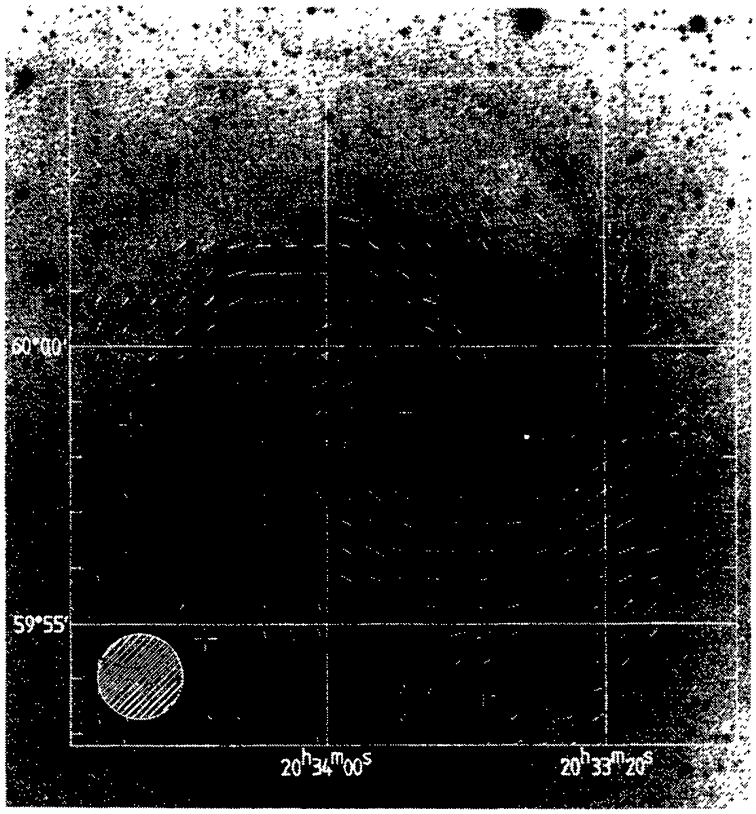

Figure 5 Magnetic field orientation in the galaxy NGC 6946 based on 2.8-cm polarization observations (Klein et al. 1982).

A Faraday rotation analysis applied to the 2.8-cm polarization data shows a clear double-peaked sinusoidal variation on the $\Delta\phi$-θ plot (Klein et al. 1982) with an amplitude of 15° at 2.8 cm. The results show that the large-scale magnetic field is in a bisymmetric spiral configuration. For the inclination $i = 30°$, the amplitude of $\Delta\phi$-θ variation corresponds to a typical $RM_0 = 1200$ rad m^{-2}, over an order of magnitude larger than the values found for M51 (60 rad m^{-2}), M81 (37 rad m^{-2}; Sofue et al. 1980), and M31 (20–30 rad m^{-2}; Sofue & Takano 1981, Beck 1982). This fact would mean that both the average strength of the uniform magnetic field and the average density of thermal electrons in NGC 6946 are possibly several times as high as those in the other galaxies. Such a conclusion is consistent with the fact that NGC 6946 has very high surface brightness in both the radio and optical, which suggests that it has a high rate of star formation. Klein et al., however, noted that the characteristic *RM* of the order of 10^3 rad m^{-2} might be too high for a spiral galaxy, and that the apparent variation of the polarization angle may be originated by some local variation of the pitch angle of the field lines deviating by $\sim 15°$ from a regular spiral. However, the observed sinusoidal deviation on the $\Delta\phi$-θ plot seems too regular to be considered a local variation.

Using a spectral index distribution, Klein et al. (1982) estimate the nonthermal contribution to the total radio emission at 2.8-cm wavelength as $19 \pm 10\%$, whereas the average polarization degree in the nonthermal emission is $10 \pm 3\%$. These values lead to a ratio between the magnetic field strength of the uniform and random components of 0.31 ± 0.06. From the energy equipartition, Klein et al. estimate that the strength of the total magnetic field is $B = 15 \pm 5$ μG, about five times as strong as the mean field strength in the solar vicinity of our Galaxy or that in M31. Klein et al. further stress that the strength of magnetic field in NGC 6946 may play a vital role in the formation of spiral arm structure.

IC 342 IC 342 is a late-type Scd spiral at low galactic latitudes ($b \approx 11°$). Optical measurements are seriously affected by the galactic dust grains, which makes it difficult to study the starlight polarization of this galaxy. A radio continuum mapping at 1.4 GHz was done with the WSRT telescope by van der Kruit (1973), and this showed a strong central source and rather low-surface-brightness distribution of the disk component with clear traces of the spiral arms, suggesting the concentration of magnetic flux in the arms. An extensive radio survey of this galaxy, including linear polarization at 6.3 and 11 cm, was done by Gräve & Beck (1986). These observations show that the electric vectors at both frequencies resemble each other and are distributed almost radially. This fact suggests that the Faraday rotation has little affect on the polarized emission, and thus that

the magnetic field may run along circular segments. In fact, a study of the variation of polarization angle at 6.3 cm along the major axis (ϕ-X plot method) is antisymmetric with respect to the center, which suggests a circular orientation of the large-scale magnetic field (Sofue et al. 1985).

OTHER SPIRAL GALAXIES The galaxies that have been mapped well enough in radio polarization to give information to determine the field configuration are limited. Using the simple ϕ-X method, Sofue et al. (1985) have derived the field configuration for several more galaxies. *NGC 253* shows a symmetric ϕ-X variation, and the large-scale field may be in a bisymmetric spiral configuration. *NGC 2903* shows a clear symmetric variation in the ϕ-X plot, which indicates a bisymmetric field configuration. *NGC 5055* possibly shows a symmetric ϕ-X variation, although the signal-to-noise ratio is not enough to give a conclusive field configuration.

The spiral galaxy *NGC 4258* is well known by its anomalous radio morphology that shows two widely open, arm-like features crossing the optical spiral arms (van der Kruit et al. 1972, de Bruyn 1977, van Albada 1978, van Albada & van der Hulst 1982, Krause et al. 1984). Sofue et al. (1980) applied the $\Delta\phi$-θ plot to the polarization data of van Albada (1978), taking care to avoid the anomalous arm regions, and derived a possible double-peaked variation suggestive of a bisymmetric spiral field configuration. However, the strong influence of the anomalous arms makes this result far from conclusive.

BARRED SPIRAL M83 (NGC 5236) The barred spiral M83 was observed at 1.5 and 5 GHz with the VLA by Ondrechen (1985). The nonthermal radio emission comes predominantly from the dark lanes along the bar and spiral arms. A significant linear polarization has been detected along the bar and spiral arms. The polarization vectors at 5 GHz, corrected for the average Faraday RM of about -40 rad m^{-2} across the bar, indicate that the magnetic field is oriented primarily along the bar. These facts are consistent with the interpretation that the bar and nonthermal spiral arms are due to a shock enhancement of the underlying disk emission (see Section 4).

We have applied the Faraday analysis to Ondrechen's 5-GHz data. The $\Delta\phi$-X plot shows a symmetric variation along the bar with respect to the center, which is consistent with a BSS field configuration. The $\Delta\phi$-θ plot also shows a double-peaked variation, again suggestive of a BSS field.

MAGELLANIC CLOUDS AND DWARF GALAXIES Recent radio continuum observations of the Magellanic Clouds have shown that the electric vectors at 1.4 GHz are distributed perpendicular to the main axis of the Small Magellanic Cloud (SMC) (Haynes et al. 1986), and this finding is not consistent with the idea that the polarization comes from the magnetic

field running between the Large (LMC) and Small Magellanic Clouds, as has been suggested from the optical polarization (Section 3.1). However, no Faraday correction, and therefore no accurate field direction, is known. No radio polarization is known for the LMC as yet.

The implication of magnetic fields in dwarf irregular galaxies like the SMC has been discussed by Klein et al. (1983b). They stress that the nonthermal characteristic is an important factor in understanding the star-forming activity and evolution of these galaxies.

3.3 *The Milky Way Galaxy*

Our Galaxy is the nearest spiral as seen edge-on from inside. Nevertheless our knowledge about the large-scale configuration of its magnetic field is rather scanty. This is because of the small depth of the optically observable space (a few kiloparsecs from the Sun) and because of the too large Faraday rotation on the radio emission, which almost completely destroys the information of linearly polarized galactic radiation after propagating the disk by tens of kiloparsecs. The popular way to derive the galactic-scale magnetic field is to use Faraday rotation measures for extragalactic radio sources like quasars and radio galaxies (Gardner & Whiteoak 1966) and those for pulsars (Manchester & Taylor 1977, Manchester 1974).

LOCAL FIELD The structure of the local magnetic field, or the field within a few kiloparsecs of the Sun, has been extensively studied in optical and radio in the past few decades and has been reviewed by Gardner & Whiteoak (1966), Heiles (1976), Spoelstra (1977), Verschuur (1979), and Vallée (1984). Since the present review concentrates on a larger-scale global field, readers may refer to these articles for the local magnetic field structure. We note here only that the average strength of the uniform component of the local field has been estimated to be 2.2 ± 0.4 μG from pulsar observations (Manchester 1974), 2 ± 1 μG from Zeeman-effect measurements (Verschuur 1974), and 3 ± 0.4 μG from the radio background intensity (Phillips et al. 1981). The authors suggest the same order of strength for the random component, which is superimposed on the uniform field.

GLOBAL FIELD By analyzing the distribution of Faraday rotation measures of quasars, radio galaxies, and pulsars, Thomson & Nelson (1980) suggested a field reversal between the local arm and the Sagittarius arm. They further argued that the magnetic field in our Galaxy may be in a bisymmetric spiral configuration running along the spiral arms, with the field direction reversing at the boundary separating the neighboring two arms. Simard-Normandin & Kronberg (1979, 1980) accumulated more *RM* data of extragalactic radio sources and analyzed the *RM* distribution.

They found that the *RM* distribution near the galactic plane is consistent with the spiral configuration, with the field direction parallel to the arms reversing its direction at the boundary separating the neighboring two arms. Sofue & Fujimoto (1983) used *RM* data collected by Tabara & Inoue (1980) to compute an *RM* distribution on the sky smoothed with a 20° HPBW Gaussian beam. They found also that the *RM* along the galactic plane changes its sign with direction of the spiral arm. The magnetic field traces the spiral arms, which are determined from the distribution of H II regions (Georgelin & Georgelin 1976). Sofue & Fujimoto (1983) further computed a model distribution of *RM*s smoothed to a 20° Gaussian beam using a bisymmetric, open-spiral configuration for the magnetic field. The observed and calculated distributions are found to resemble each other.

In contrast to these *RM* analyses, which suggest a bisymmetric spiral field configuration, Vallée (1983a,b) insists that the global field must be circular from the fact that the local field is directed toward $l = 90$–$100°$ (Inoue & Tabara 1981), a direction consistent with the gas flow in the galactic shock-wave model for spiral arms (Roberts & Yuan 1970): In the interarm region, the flow lines and therefore the field lines are rather oriented in a leading sense. This field configuration is, however, inconsistent with that inferred from the field component projected on the sky in external galaxies (Figures 3–5).

3.4 *Magnetic Halo*

The magnetic halo significantly affects our understanding of the origin and magnetohydrodynamic behavior of the magnetic field in the disk (see Section 4). Our knowledge of magnetic fields in halos is still rather poor because of the lack of linear polarization observations of the faint extended components apart from disk planes. However, the existence of nonthermal radio emission significantly extended above the disk planes in several edge-on galaxies indicates the existence of magnetic halos.

EDGE-ON GALAXIES

NGC 3079 A 20-cm map of this almost edge-on galaxy (de Bruyn 1977) exhibits an extended radio halo over ~ 1 kpc above the galactic plane. A recent VLA map of this galaxy (Duric et al. 1983) reveals lobe structures extending over 2 kpc from the nucleus, perpendicular to the galactic plane. The lobes are significantly polarized at 6 and 20 cm, which indicates the magnetic fields. Duric et al. suggest that the lobes may be due to the activity at the central region of this galaxy, which ejects magnetic bubbles perpendicular to the disk plane. An interaction of the ejecta with the halo materials, one involving magnetic fields, may have caused a strong shock that enhances the field strength to give the high degree of linear polarization in the lobes.

NGC 891 This is an edge-on galaxy having a halo component in the radio continuum (Allen et al. 1978, Beck et al. 1979, Klein et al. 1984). The field strength as estimated from the equipartition assumption is of the order of a few microgauss at ~ 5 kpc above the galactic plane (Allen et al. 1978).

NGC 253 This is an irregular spiral of large inclination. A 10.7-GHz map of this galaxy (Klein et al. 1983a) and a 1.4-GHz map (Hummel et al. 1984b) reveal a halo extending up to 5 kpc above the galactic plane surrounding the center. The field strength as estimated from the equipartition assumption is again of the order of a few microgauss at 2–3 kpc above the galactic plane.

NGC 4631 This edge-on galaxy has also been shown to have a nonthermal radio halo (Ekers & Sancisi 1977, Wielebinski & von Kap-herr 1977, Klein et al. 1984), which suggests the existence of a magnetic field. From radio continuum observations at four frequencies (0.6, 1.4, 4.8, and 10.7 GHz), Werner (1985) has shown a clear indication of a nonthermal halo with a "1% level thickness" of about 5 kpc from the galactic plane. He concludes that the frequency dependence of the radio emission above the disk supports a dynamical halo model.

More examples of edge-on galaxies having a thick disk or a halo have been reported by Hummel et al. (1984a). However, the observational data are still too crude to put severe constraints on the existing models of the galactic halo (see Section 5). The number of edge-on galaxies studied to date is still too small to ascertain whether magnetic halos are common among spiral galaxies.

OUR GALAXY The existence of a hot gaseous halo surrounding the Galaxy with a scale height of several kiloparsecs has been established with optical and UV observations (Spitzer 1956, Savage & de Boer 1979, 1981, York, 1982). The existence of a magnetic halo has been a long-standing question (Baldwin 1959) because of its important connection to the leakage problem of cosmic rays and their lifetime (Webster 1975, 1978, Wielebinski 1983). An attempt to unfold the 408-MHz survey data of the galactic radio continuum background has shown the existence of a thick disk indicative of a magnetic halo with cosmic rays (Phillips et al. 1981, Beuermann et al. 1985).

A more convincing indication of a halo field is shown by a statistical analysis of Faraday rotation of extragalactic radio sources and pulsars; such an analysis is performed by plotting their $|RM|$ against cot $|b|$, where b is the galactic latitude. The upper envelope of the distribution of the sources on the $|RM|$–cot $|b|$ plane is well represented by the relation

$$|RM| = RM_0 \cot |b|. \qquad 3.1$$

This b-dependence of RM is due to a plane-parallel distribution of magnetic field and ionized gas in the Galaxy. The coefficient RM_0 for extragalactic sources has been obtained as $RM_0(\text{ext}) \cong 30$ rad m^{-2} (Sofue et al. 1979, Inoue & Tabara 1981). On the other hand, the RM_0 obtained for pulsars (Manchester & Taylor 1977) is significantly smaller: $RM_0(\text{psr}) \cong 10$ rad m^{-2} (Sofue et al. 1979). Since pulsars are distributed below 500 pc from the galactic plane, the remaining galactic contribution to the extragalactic sources, $20[\cong RM_0(\text{ext}) - RM_0(\text{psr})]$ cot $|b|$ rad m^{-2}, must be due to a galactic halo beyond ~ 500 pc from the galactic plane. If we tentatively assume a halo thickness of the layer responsible for the Faraday rotation as ~ 3 kpc and the electron density as 10^{-3} cm^{-3} (Savage & de Boer 1979), the field strength in the halo is estimated to be of the order of a few microgauss. This amount is consistent with those values obtained for the halo field in edge-on galaxies (see Section 3.2).

4. THEORETICAL ASPECTS OF THE RING AND BISYMMETRIC SPIRAL MAGNETIC FIELDS

The "ring" and "bisymmetric spiral" are two main global configurations of magnetic fields that fit the observations of nearby spiral galaxies. The majority of spiral galaxies have the BSS magnetic fields (Table 2). The present section surveys the theoretical papers on the ring and BSS fields in spiral galaxies. Since the latter field configuration has been only very recently discovered, only a few papers about it have been published so far. Section 4.3 is presented therefore as material for understanding the BSS field configuration. More general discussions about the dynamics of local magnetic fields in galaxies and the Galaxy may be found in Chandrasekhar (1961), Piddington (1969), Moffat (1978), Parker (1979), Zeldovich et al. (1983), and Begelman et al. (1984).

4.1 *Ring Magnetic Fields*

This magnetic field configuration was considered soon after the optical polarization of starlight was extensively measured in the solar neighborhood (Hiltner 1956, 1958). It is quite natural to consider that the spiral arm is approximated by a ring, with the interstellar magnetic lines of force parallel to it. Radio observations by Morris & Berge (1964) suggested the longitudinal model of magnetic field along the ring arm.

Chandrasekhar & Fermi (1953) discussed the gravitational instability of a conducting liquid cylinder with a longitudinal magnetic field. Their paper was a basis for further studies of the dynamical problems of a cylindrical conducting medium both in astronomy and in laboratory plasma physics. Pacholczyk (1963) treated ring-like or circular magnetic

fields in conducting gas in galactic rotation. A stability effect of magnetic fields has been clarified in relation to the differential rotation, which is one of the most important dynamical characteristics of spiral galaxies.

Elvius & Herlofson (1960) were the first to work on some details of the ring magnetic field in galaxies. They predicted a different dynamical behavior for interstellar gas as compared with young stars by taking into account the curvature force of the ring magnetic field. This model was, without being tested observationally, soon replaced by the star formation scenario in the galactic spiral shock-wave theory.

A modern development of the ring magnetic field was initiated by Parker (1971a,b). He treated turbulent diffusion of magnetic fields and the dynamo action due to the cyclonic turbulence or to the coupling between the turbulence and the galactic rotation. These two processes are still very open to further theoretical (turbulent diffusion) as well as observational (cyclonic turbulence) studies. Nevertheless, the rational scenario of the ring model is realistic enough to apply to the magnetic field problems in spiral galaxies. Thus, a number of papers have been published on the dynamo action. The present understanding of the ring-like magnetic field in a galaxy seems rather coherent [Vainshtein & Ruzmaikin 1971, Levy 1974, Stix 1975, 1976, Deinzer 1976, Soward 1978, White 1978, Schüssler 1979, Ruzmaikin et al. 1980, 1985, Ruzmaikin & Shukurov 1981, Pismis 1984; see also Cowling (1981) for a discussion of dynamo processes in other astronomical objects]. On the other hand, Layzer et al. (1979) have seriously questioned the conventional treatments of the diffusion of passive magnetic fields in a turbulent medium and the decay of the fluctuated field component.

The ring field, suggested as the most probable field configuration in M31 (Section 3.2), seems to be well within the scope of dynamo theory of the axisymmetric magnetic field. Since this theory can be extended further to apply to the BSS fields in the majority of spiral galaxies, we briefly touch upon the induction-and-dynamo process in a thin disk of finite thickness in differential rotation (Parker 1971a,b, 1975). The induction-and-dynamo equation for the mean field $\mathbf{B}$ is

$$\frac{\partial \mathbf{B}}{\partial t} = \mathrm{rot}\,(\mathbf{u} \times \mathbf{B}) + \eta \nabla^2 \mathbf{B} + \mathrm{rot}\,(\Gamma \mathbf{B}) \qquad 4.1$$

and

$$\mathrm{div}\ \mathbf{B} = 0, \qquad 4.2$$

where η is the magnetic diffusion (dissipation) constant due to the turbulent motion superimposed on the galactic rotation $\mathbf{u}$. The dynamo strength is represented by Γ, which is a matrix in general but it is treated here as a

scalar for simplicity without loss of accuracy (Zeldovich et al. 1983). [For a matrix form of Γ, see Parker (1970) and Moffat (1970).] In cylindrical coordinates (r, ϕ, z), we have $\mathbf{u} = [0, V(r), 0]$ and $\mathbf{B} = [B_r(r,z), B_\phi(r,z), B_z(r,z)]$ in which all components are independent of ϕ (the direction of galactic rotation). When we take the local rectangular coordinates (x, y, z), whose origin rotates with the disk matter, Equations 4.1 and 4.2 are approximated as

$$\frac{\partial B_x}{\partial t} = \eta\left(\frac{\partial^2 B_x}{\partial x^2} + \frac{\partial^2 B_x}{\partial z^2}\right) + \frac{\partial}{\partial z}\Gamma B_y, \tag{4.3}$$

$$\frac{\partial B_y}{\partial t} = \eta\left(\frac{\partial^2 B_y}{\partial x^2} + \frac{\partial^2 B_y}{\partial z^2}\right) + \frac{\partial V}{\partial x} B_x, \tag{4.4}$$

$$\frac{\partial B_z}{\partial t} = \eta\left(\frac{\partial^2 B_z}{\partial x^2} + \frac{\partial^2 B_z}{\partial z^2}\right) - \frac{\partial}{\partial x}\Gamma B_y, \tag{4.5}$$

and

$$\frac{\partial B_x}{\partial x} + \frac{\partial B_z}{\partial z} = 0, \tag{4.6}$$

where the x axis is directed to the galactic anticenter, the y axis to the galactic rotation, and the z axis parallel to the symmetry axis of the disk. The curvature of the field line is small and neglected. The field generation in the y axis along the galactic rotation is dominated by the differential rotation.

A solution in the form of $\mathbf{B} = \mathbf{b} \exp i(-\omega t + k_x x + k_z z)$ is substituted into Equations 4.3–4.5. A dispersion equation can then be obtained, namely

$$(k_x^2/k^2 + k_z^2/k^2 - i\omega/\eta k^2)^2 - ik_z/k = 0, \tag{4.7}$$

where $k = 3(G\Gamma/\eta^2)^{1/2}$ with $G \equiv (dV/dx - V/r)_{x=0}$. When we presume $k_x = m$ as given, the dispersion equation (4.7) is reduced to the relation between ω and k_z. We have four roots for k_z (n_1, n_2, n_3, and n_4). Thus, the general solution of Equations 4.3–4.5 can be represented by a superposition of four plane waves;

$$\mathbf{B} = \sum_{j=1}^{4} \mathbf{b}_j \exp i(-\omega t + mx + n_j z). \tag{4.8}$$

The angular frequency ω and the amplitudes $\mathbf{b}_j$ $(j = 1, 2, 3, 4)$ are to be determined as an eigenvalue problem under a set of boundary conditions such as those given in Figure 6. A result is shown in the magnetic field

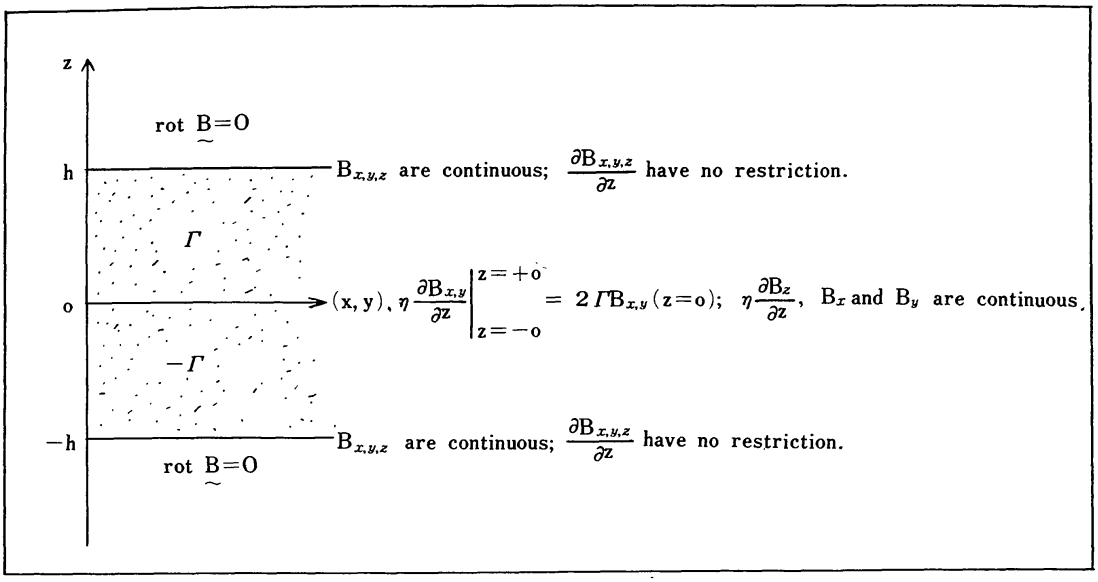

Figure 6 Boundary conditions of the magnetic field components at the central plane ($z = 0$) and the upper and lower surfaces of the disk ($z = \pm h$).

distribution in Figure 7, which is for the BSS field case in Section 4.3 but is locally very similar to the ring field case. The dynamo theory predicts that besides the ring field in the disk, the upper parts of the disk and the space outside of it are dominated by a poloidal field. The growth time of this field configuration is $\sim 10^8$ yr for the thin disk of thickness $2h = 200$ pc, dynamo strength $\Gamma = 0.5$ km s^{-1}, and turbulent diffusion constant $\eta = \frac{1}{3} \times 10$ km s$^{-1} \times 100$ pc. The above growth/decay time of the field configuration can be also estimated by the energy principle (Levy 1974) even without knowing the eigenfunction $\mathbf{b}_j$ ($j = 1, 2, 3, 4$).

The turbulent diffusion of the magnetic field remains open to further theoretical investigations (Layzer et al. 1979). However, it has successfully solved many problems about magnetic fields in various astronomical

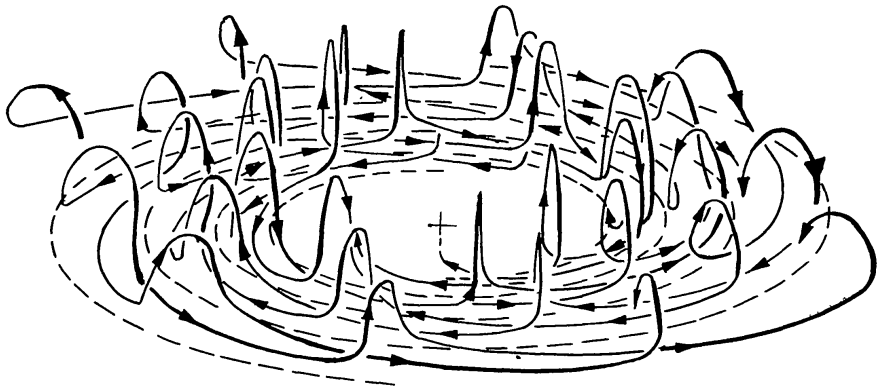

Figure 7 Global distribution of the BSS magnetic field (Fujimoto & Sawa 1986).

objects. Thus, the turbulent and dynamo model for the ring magnetic field has become increasingly accepted in this decade. Another attractive point is that this ring field model can be applied without meeting the difficulty of the secular winding-up of the magnetic lines of force, and (as is discussed in Section 4.2) no discrepancy has yet been found with observations.

RING MAGNETIC FIELDS AND THEIR ALIGNMENT ALONG THE SPIRAL ARMS

The galactic spiral shock wave is a coherent and basic process in the disk gas of spiral galaxies (Fujimoto 1966, Roberts 1969). Interaction of the ring magnetic field with this spiral shock wave has been studied by Roberts & Yuan (1970) and Tosa (1973). They took the nonlinear hydromagnetic equation and the shock-front conditions at the spiral potential-well, which are essentially the same as those employed by the former two authors. The magnetic fluxes parallel to the shock front are condensed, whereas the perpendicular component to it remains unchanged. As a result, the field lines are observed to be locally maximal in the arm and aligned to it. Such a field alignment is entirely consistent with observations in galaxies and in the solar neighborhood of the Galaxy. In this case, the "ring" field is somewhat distorted by the noncircular galactic rotation of gas due to the spiral gravitational potential, but it is still closed in the disk plane (Vallée 1983a).

4.2 *Bisymmetric Spiral (BSS) Magnetic Fields*

The majority of spiral galaxies exhibit the BSS field, except for cases such as M31 and IC 342, which are suggested to have a ring field configuration (Table 2). Since this trend seems to hold for most spiral galaxies, the ring field model described in Section 4.1 is not enough to understand the global magnetic field in spiral galaxies. In fact, the BSS field is topologically different from the ring field, i.e. no physically permissible transformation is known from the ring field configuration to the BSS.

In contrast to the ring field, the BSS field configuration favors a primordial origin of magnetic fields (Piddington 1969, Tosa & Fujimoto 1978). The primordial origin hypothesis considers that an intergalactic ordered magnetic field was captured into a protogalaxy, contracted, twisted up by the differential rotation to form the BSS field, and maintained up to the present time by some "mechanism" (see Figure 10*a*). Vallée (1983a,b) claims legitimately that we can accept neither the BSS field nor the primordial origin hypothesis unless we have a competing theoretical model with the physics of this "mechanism" correctly treated in a quantitative way. In this sense, the hydromagnetic models for spiral arms developed earlier than 1965 (Wentzel 1960, Hoyle & Ireland 1961, Pismis 1960, Ohki et al. 1964) cannot be applied for the present BSS field.

Recently Sawa & Fujimoto (1986) and Fujimoto & Sawa (1986)

extended Parker's (1971a,b) induction-and-dynamo model and applied it for the BSS magnetic field in spiral disk galaxies. The employed equations are the same as Equations 4.1 and 4.2, except that we now have, contrary to the ring field, $\mathbf{B} = [B_r(r, \phi, z), B_\phi(r, \phi, z), B_z(r, \phi, z)]$. Since we use Equation 4.1 in the rest frame, $\mathbf{u}$ is the galactic rotation $\mathbf{u} = [0, V(r), 0]$. An asymptotic solution is searched for in the spiral distribution of magnetic field in the form of

$$\mathbf{B} = \mathbf{b}(r) \exp i(-\omega t + \phi + k_z z + \ln r/\delta), \tag{4.9}$$

where the amplitude $\mathbf{b}(r)$ is a slowly varying function of r. In the argument of the exponential function, $\phi + \ln r/\delta = \text{constant}$ describes a logarithmic spiral $r = e^{\delta\phi}$ that traces approximately the luminous arm and the BSS magnetic lines of force when δ is small (say $\delta = 0.1$). The wave number in the z direction, k_z, is allowed to be complex, and the scale height of the field distribution is $1/\mathrm{Im}(k_z)$.

Using this small number δ, we expand $\mathbf{b}(r)$ in a power series

$$\mathbf{b}(r) = \mathbf{c}_0(r) + \mathbf{c}_1(r)\delta + \mathbf{c}_2(r)\delta^2 + \ldots. \tag{4.10}$$

Substituting Equations 4.9 and 4.10 into Equations 4.1 and 4.2 and taking the dominant terms, we have a set of equations very similar to Equations 4.3–4.6. However, we have additive terms due to $(\mathbf{u}\cdot\nabla)\mathbf{B}$ in Equation 4.1. (Note that Equations 4.4–4.6 are described in the rotating local rectangular coordinates.) The dispersion relation for the BSS field distribution (Equation 4.9) is given by

$$(1/k^2\delta^2r^2 + k_z^2/k^2 + iV/\eta k^2 - i\omega/\eta k^2)^2 - ik_z/k = 0, \tag{4.11}$$

where $k = (G\Gamma/\eta^2)^{1/3}$ and $G \equiv dV/dr - V/r$. Equation 4.11 corresponds to Equation 4.7 for the ring field and reduces to Equation 4.7 when $1/\delta^2r^2 = k_x^2$ and $V = 0$. In the dispersion equation (4.11), r and its functions are regarded as only slowly varying against r or practically constant. This mathematical procedure reminds us of the spiral density-wave analysis (Lin & Shu 1964): The BSS magnetic field is obviously a global and coherent phenomenon, but the basic process needed to generate and sustain it can be described by the local process.

The dispersion relation (4.11) gives four roots for k_z against ω, namely n_1, n_2, n_3, and n_4. Thus the general solution is written as a superposition of four spiral waves,

$$\mathbf{B}(r, \phi, z) = \sum_{j=1}^{4} \mathbf{b}_j(r) \exp i(-\omega t + \phi + n_j z + \ln r/\delta), \tag{4.12}$$

with Equation 4.12 corresponding to Equation 4.8. The amplitudes $\mathbf{b}_j$

($j = 1, 2, 3, 4$) and the angular frequency ω can be determined as an eigenvalue problem in the same way as in the ring field model in Section 4.1.

A result is given in a magnetic field distribution diagram in Figure 7, where we have assumed a "thick" disk with $2h = 1$–1.5 kpc, a stronger dynamo action with $\Gamma = 2.5$ km s^{-1}, and other parameters the same as those in the ring field model. We find that the region of local maximum field traces two spirals on the galactic plane ($z = 0$), and that the magnetic field reverses its direction across the boundary of the two spirals. The field distribution in the lower half of the disk ($z < 0$) can be reproduced by making the mirror-symmetric transformation of Figure 7 with respect to $z = 0$. In the upper part of the disk and partly in the outer space, the poloidal component becomes dominant, making a helical structure when projected onto the meridional plane.

If the various quantities are normalized to the parameters of the Galaxy, the outer radius of the spirals in Figure 7 corresponds to 13 kpc. This field pattern rotates rigidly with angular velocity $2\pi/\mathrm{Re}(\omega) \simeq 10$ km s^{-1} kpc^{-1}. The magnetic field grows with a time scale of $2\pi/\mathrm{Im}(\omega) \simeq 1.5 \times 10^9$ yr. We can thus conclude that the induction-and-dynamo process reproduces the BSS magnetic field in the galactic-disk gas as a quasi-steady pattern that is not further twisted by the differential rotation. It must be stressed that the BSS field is a global and coherent phenomenon closely related to the thicker disk of magnetic fields and/or to the galactic halo. In fact, the adopted thicker disk ($2h = 1$–1.5 kpc) causes a dynamo strength 3–5 times as large as that evaluated in the thin disk ($2h = 200$ pc) by Parker (1971a,b).

Since the 1970s, several theoretical models of the double spiral arms have been introduced with the magnetic field aligned to the arms. Kaplan & Pickelner (1970) and Akasofu & Hakamada (1982) noted a certain similarity between the gas dynamics of spiral galaxies and of the solar wind and the Archimedean spiral magnetic line of force. According to Akasofu & Hakamada's (1982) heliospheric model, double spiral condensations of gas and magnetic fields result if the galactic gas has a radially outward motion of 10 km s^{-1}, with two maxima separated by 180° in longitude. As Vallée (1982) argued, however, the predicted magnetic field distribution is entirely inconsistent with that observed in the solar neighborhood. Furthermore, if the outward-streaming gas locally follows the observed galactic rotation, the resultant spiral condensations of gas and magnetic fields are extremely tightly twisted and are obviously incompatible with observation. This heliospheric model could be applied to the stronger magnetic fields in more active spiral galaxies such as NGC 4258 (van Albada 1978) and in galactic nuclei.

Piddington (1969, 1978, 1981) has long stressed the important role of primordial magnetic fields in the gas dynamics of galaxies. Although our

BSS fields are topologically consistent with his double spiral fields, it still seems difficult to accept his fields in their present form, since no known mechanisms can sustain these double spiral magnetic fields for a period of 10^9–10^{10} yr.

The induction-and-dynamo process for the BSS magnetic field seems the most realistic at present, and we thus feel that the magnetic fields in the majority of spiral galaxies are of primordial origin. However, many problems must be solved in the future. The nearby spiral galaxies, designated by the symbol "BSS" in Table 2, satisfy the characteristic conditions of the bisymmetric spiral magnetic field in that the RM-θ and $\Delta\phi$-X plots show double-peak variation (Section 2). Beck et al. (1985) found that the amplitude of the sinusoidal angle distribution remains the same at wavelengths of 6 and 21 cm for M81. This result cannot be explained strictly by Faraday rotations due to a BSS field: The Faraday amplitude at 6 cm must be reduced to one tenth of that at 21 cm. The position angles of the observed E vectors in M81 could represent the intrinsic polarization vectors caused by a more complicated field configuration. The same argument might explain the too large amplitude obtained for NGC 6946 (Klein et al. 1982). In any case, these observational data supply new material for the next step in the theoretical model for the BSS magnetic field. More data with good angular resolution and dynamical range are necessary.

4.3 *Global Magnetic Fields in the Galactic Halo*

The presence of magnetic fields in the halo of ~ 1 μG has been indicated by observations of nonthermal radio emission extended far above the disks in some galaxies; the global configurations of these fields, however, are not known (Section 3). As discussed in Sections 4.2 and 4.3, the disk fields extend high above the disk and diffuse into the halo. In view of our discussions so far, we note that observational as well as theoretical data about the global magnetic fields in the halo are very poor and only fragmentary. The following theoretical arguments are therefore only to be taken as trial explanations for the global picture of magnetic fields in the galactic halo.

Lipunov (1979) considered the interaction between accreting intergalactic gas and the magnetic field of the Galaxy. If the field strength of the galactic halo is $(3\text{–}5) \times 10^{-7}$ G and the accreting gas density is $(1\text{–}3) \times 10^{-29}$ g cm^{-3}, a flat magnetosphere (halo) of the Galaxy is generated at a distance $|z| = 5$–8 kpc from the galactic plane. Therefore the undisturbed magnetic field is specified by a law of $B = 2(z/h)^{-K}$ μG, where $1/2 < K < 3/4$ and $2h$ represents the thickness of the disk. The field strength decreases outward more slowly than that expected for the dipole magnetic field.

Mikhailov & Syrovatskii (1980) proposed that the regular magnetic field component in the galactic halo could be detected by measuring the characteristic arrival direction of ultra-high-energy particles of more than 10^{17} eV and the polarization of synchrotron radiation. The halo field in the solar neighborhood was thus obtained as 3 μG directed along $l = 270°$, opposite to the field direction in the disk.

As Bregman (1980, 1981) and Habe & Ikeuchi (1980) noted, a complex motion of gas occurs as a result of a "galactic fountain"–type flow; hot gas heated by supernovae and newly born stars is accelerated upward from the disk. Some of the gas flows out into intergalactic space, whereas some of the gas cools, condenses, and returns to the disk in ballistic orbits. Such a rising-and-falling motion of gas has indeed been found above the spiral arms of some galaxies (Tosa & Sofue 1974, Sofue & Tosa 1974). The gas of the galactic halo will therefore be in a dynamic and chaotic state, with the magnetic field being highly tangled. Numerous magnetic loops may be stretched out of the disk.

The halo gas rotates more slowly than the disk gas, and its density is 10^{-3} (H atom) cm^{-3} (de Boer & Savage 1983). If the magnetic stress in the halo becomes comparable to the kinetic-energy density of the gas, tightly twisted field lines in the halo may be relaxed. Sawa & Fujimoto (1980) and Fujimoto & Sawa (1981) considered a magnetic interaction between the halo and disk gases, by which the BSS field can be maintained in the disk in differential rotation. The field lines in the halo are taken to be parallel to the disk and sustained in a bisymmetric open-spiral state.

We have surveyed several papers on the global magnetic field in the halo, but the papers on this topic show little consensus as yet except for the prediction of a field strength of ~ 1 μG in the halo. Observations of linearly polarized emission from the halo and the upper parts of the radio disk of edge-on spiral galaxies are urgently needed for constructing a model of the halo magnetic field.

4.4 *Magnetic Field Structure in Other Types of Galaxies*

BARRED GALAXIES Recent VLA observations by Ondrechen (1985) of the barred spiral galaxy M83 show a large-scale magnetic field parallel to the spiral arms in the outer regions and to a pair of dust lanes on the leading sides of the bar (Section 3.2). Ondrechen (1985) concluded that these facts are consistent with the strong noncircular motion of gas having a passive magnetic field and with the resultant shock waves in the bar. These characteristic motions of gas in SB galaxies have been extensively studied by Sorensen et al. (1976), Roberts et al. (1979), and Sanders & Tubbs (1980). [See also Sanders & Huntley (1976) for the outer response of gas to the rotating bar potential.]

Our preliminary analysis of the polarization vectors at 5 GHz presented by Ondrechen (1985) suggests that the global configuration of the magnetic field in M83 is more likely BSS than ring-like. One possible model is that a BSS magnetic field, originally in the outer spiral arm region, was transported to the inner-bar region by the gas, which is drifting toward the center by losing its angular momentum at the dust lanes or at the galactic shock waves. (See the references quoted above for the loss of angular momentum at the shock waves.)

DWARF GALAXIES Radio continuum observations were initiated recently of several dwarf galaxies (Klein et al. 1983b). Nonthermal emission was detected, indicating the presence of magnetic fields, but no polarization measurements have yet been made.

If dwarf galaxies rotate rigidly, no BSS magnetic field can be expected because of the lack of differential rotation. Instead, we could suppose a dipolar configuration of the magnetic field such as in the Earth, Jupiter, and the Sun, all of which are rigid rotators. The magnetic field is sustained by the dynamo action due to the gas in convective motion at the centers of dwarf galaxies, where newly born stars strongly disturb the ambient gas.

5. ASTRONOMICAL IMPLICATIONS OF THE LARGE-SCALE MAGNETIC FIELDS IN SPIRAL GALAXIES

We have reviewed observations and theories of the large-scale configuration of magnetic fields in spiral galaxies. Both the ring and BSS field configurations have been found in nearby spiral galaxies, and both configurations are shown theoretically to be generated and/or maintained by the turbulent diffusion and the dynamo action in a galactic disk of finite thickness with differential rotation. In particular, the BSS field is regarded as a magnetic field pattern rotating rigidly without being twisted by differential rotation.

5.1 *The Primordial Origin of the BSS Magnetic Field*

The BSS topology supports the primordial origin hypothesis for magnetic fields in spiral galaxies. In this hypothesis, the intergalactic ordered field was captured by a protogalaxy and then contracted and twisted by the differential rotation to generate a BSS field (see Figure 10*a*). It has been maintained since then by the induction-and-dynamo process. We note, however, that although the BSS configuration is due to the primordial origin, the magnetic fluxes are generated after the formation of the galaxy.

The ring field in M31 is due to dynamo action. However, the seed for

the ring field is still open to discussion. (See Section 5.6 for a discussion of possible primordial origin for the ring field.)

5.2 *Spiral Condensations of Gas in the BSS Field*

The BSS field in the disk ($z = 0$) is represented in the form

$$\mathbf{B}(r, \phi, 0; t) = \mathbf{b}(r) \exp i(-\omega t + \phi + \ln r/\delta) \qquad 5.1$$

(see Equation 4.12). The Lorentz force $\mathbf{j} \times \mathbf{B} = \text{rot } \mathbf{B} \times \mathbf{B}/4\pi$ has the diadics $\mathbf{BB} \propto \exp 2i(\phi + \ln r/\delta)$, which is BSS in an exact sense. The Lorentz acceleration, although much smaller than the background gravitational force, perturbs the disk gas strong enough to generate two spiral condensations of gas along the neutral lines (Fujimoto & Tosa 1980). We then have

$$\frac{\delta\rho}{\rho} \propto \exp i(2\phi + 2 \ln r/\delta), \qquad 5.2$$

where ρ and $\delta\rho$ are the unperturbed and perturbed densities of gas, respectively. We obtain $0.01 < |\delta\rho/\rho| < 0.4$ for the numerical ranges of parameters [i.e. $|\mathbf{B}| = (3\text{–}15)\ \mu\text{G}$ and $\rho = (0.5\text{–}3)$ (H atoms) cm^{-3}].

The magnetohydrodynamical formation of the gaseous spiral arms occurs in the disk of the BSS field. It is not clear, however, whether these nongravitational spiral arms are identical with those of density-wave theory. They may be distinguished by the observed geometries of the neutral lines of the BSS field and of the luminous spiral arms.

5.3 *Large-Scale Motion of Gas and the BSS Field*

A steady or a quasi-steady BSS magnetic field is sustained at the cost of its diffusion into the halo and probably into intergalactic space. This energy loss is compensated for by the galactic rotation energy or the potential energy of the disk gas. The balance equation for these energies in a circular strip whose radius is r and width Δ is given by

$$2\pi r\Delta \frac{B^2}{8\pi} \frac{1}{2T} = 2\pi r\Delta \frac{d}{dt}\left(\frac{1}{2}\rho V^2\right), \qquad 5.3$$

$$= 2\pi r\Delta \frac{d\Phi}{dr} \frac{dr}{dt},$$

where T is the period of the galactic rotation at r, and $d\Phi/dr$ is the radial gradient of the background gravitational potential, which balances the centrifugal force $d\Phi/dr = -V^2/r$. The drifting velocity dr/dt is induced by the loss of the kinetic energy. It is written in terms of V and the Alfvén

velocity V_A as

$$\frac{dr}{dt} = -\frac{V_A^2}{2\pi V}. \qquad 5.4$$

In shocked spiral arms, we may take $V_A \sim 30$ km s^{-1}. We then have $dr/dt \simeq -1$ km s^{-1} for $V = 200$ km s^{-1}. This inward velocity seems very small, but the gaseous component moves over the disk scale in 10^{10} yr. A large-scale condensation of gas toward the center is thus expected to be controlled by the BSS field.

5.4 *Evolution of a Gaseous Disk*

The dynamo strength Γ in Equation 4.1 is taken to be a constant. However, Γ certainly depends on the strength of interstellar turbulence. Suppose that Γ increases for some reason, say by a temporary enhancement of the turbulent motion due to star formation and supernova explosions; then the field is amplified and tends toward another (magnetically) high-energy steady state. This stronger field will cause an increase of the inward drift of gas given by Equation 5.4. The gaseous component contracts toward the center more rapidly, which leads to more active star formation and a higher rate of supernova explosions. The interstellar gas is disturbed, which increases the turbulent motion and consequently the dynamo strength Γ. Figure 8 illustrates the cyclic relation among these effects.

Note, however, that the increase in B in turn suppresses the growth of the turbulence, which decelerates the cyclic process as a whole. Also, the increase in ρ leads to the decrease of V_A and therefore decelerates the inward motion (Equation 5.4), and thus the cyclic action slows down. In this way, the process in Figure 8 with the BSS field is likely controlling the global evolution of gas in a disk galaxy.

As can be seen in Figure 8, this process predicts an interrelation among

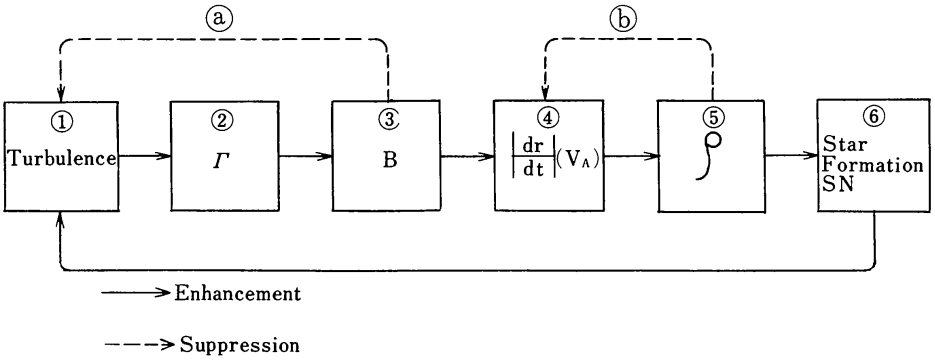

Figure 8 Cyclic process in a disk galaxy controlled by a BSS field. (*a*) Increase in B suppresses turbulence. (*b*) Increase in ρ leads to a decrease in V_A, the local Alfvén velocity.

various observable quantities like B, ρ, the optical/infrared luminosity ratio (star-forming activity), and nonthermal radio emission (supernova rate) in galaxies. In the following, we discuss some examples of these relationships.

5.5 *Star Formation and Magnetic Field in Galaxies*

The close correlation between the magnetic field and star-forming activity in spiral galaxies has been suggested by various statistical data, such as those on the radio luminosity–optical magnitude relationship (Hummel 1980, 1981, Klein & Emerson 1981) or on the radio luminosity–optical color relationship (Klein 1982). The correlation between radio flux and far-infrared flux confirms this idea (de Jong et al. 1985, Wunderlich 1985, Helou et al. 1985). An example of a more direct relation between processes 3 and 5 in Figure 8 is shown in Figure 9, where we plot the face-on CO intensity I_{CO} against magnetic field strength B_t for several galaxies. From the plot we map the line

$$B_t^2\ (\mu\mathrm{G}) = 20\, I_{CO}\,(\mathrm{K\ km\ s^{-1}}), \tag{5.5}$$

which is a correlation between the field strength and the content of molecular hydrogen gas.

This relationship can be interpreted as stating that the turbulent velocity of the interstellar gas is constant in spiral galaxies. The equipartition of energy between the magnetic field and the interstellar gas is written as

$$B_t^2/8\pi = (1/2)\rho v_t^2 = (1/2)\sigma v_t^2/h_g, \tag{5.6}$$

where ρ and σ are the volume and surface densities, v_t is the turbulent velocity, h_g is the thickness of the gas layer, and σ is given by $\sigma\ (M_\odot/\mathrm{pc}^2) = 5.8\ I_{CO}$ (K km s^{-1}) (Solomon 1983). From Equation 5.6, we have $B_t^2 = 4\pi v_t^2\sigma/h_g$, where $4\pi v_t^2/h_g$ is exactly the coefficient of the proportionality relationship in Equation 5.5 and v_t^2 is constant when the thickness of the gas layer is constant.

5.6 *Origin of Galactic Magnetic Fields and the Intergalactic Magnetic Field*

The BSS field observed in many spiral galaxies strongly suggests the existence of a primordial intergalactic magnetic field at the epoch when the galaxies formed. In fact, evidence for an intergalactic magnetic field of the order of 1 nG has been suggested (Fujimoto et al. 1971, Sofue et al. 1979, Weller et al. 1984). It is likely that a protogalaxy winds up such a larger scale field when it contracts (see Section 4.3 and Figure 10*a*).

As discussed, many investigators have assumed that the ring field is not

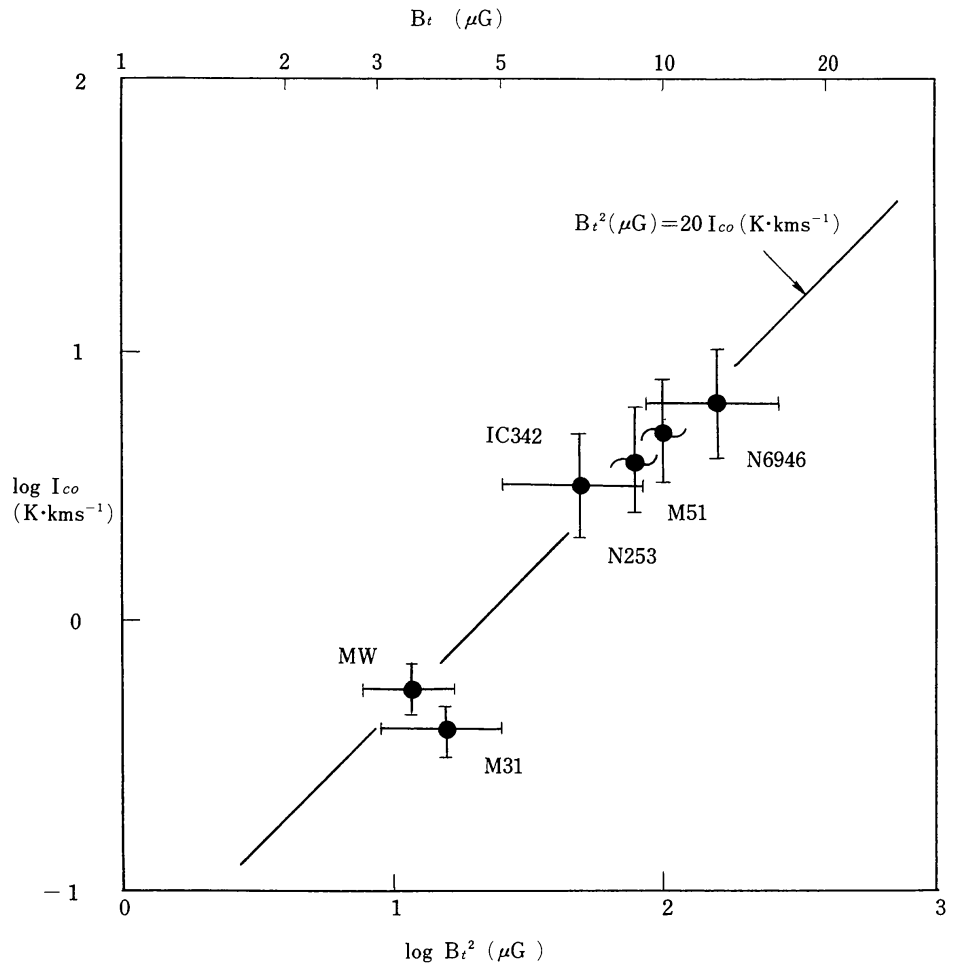

Figure 9 Relation between magnetic field strength and face-on CO intensity I_{CO}. B_t was taken from Beck (1983), I_{CO} from Solomon (1983) for M31 (value at $R = 5$ kpc), NGC 6946 (5 kpc), IC 342 (5 kpc) and M31 (10 kpc), and from Scoville et al. (1985) for NGC 253 (3 kpc).

due to a primordial origin but rather to the dynamo action, and for M31 this seems to be the case (Section 4.1). However, such a topological evolution of magnetic lines of force, as illustrated in Figure 10, indicates that a ring field is generated from a primordial field that was trapped by a protogalaxy in an asymmetrical way with respect to the center. If the reconnection of the field lines occurs as a result of the turbulent diffusion, a closed ring field is produced in the inner part of the galaxy that is associated with an open BSS field in the outer part. Since such an asymmetric field distribution at the protogalactic stage and the subsequent field annihilation are sufficiently realistic, we should consider both the dynamo and primordial origins for the ring field with equal weight.

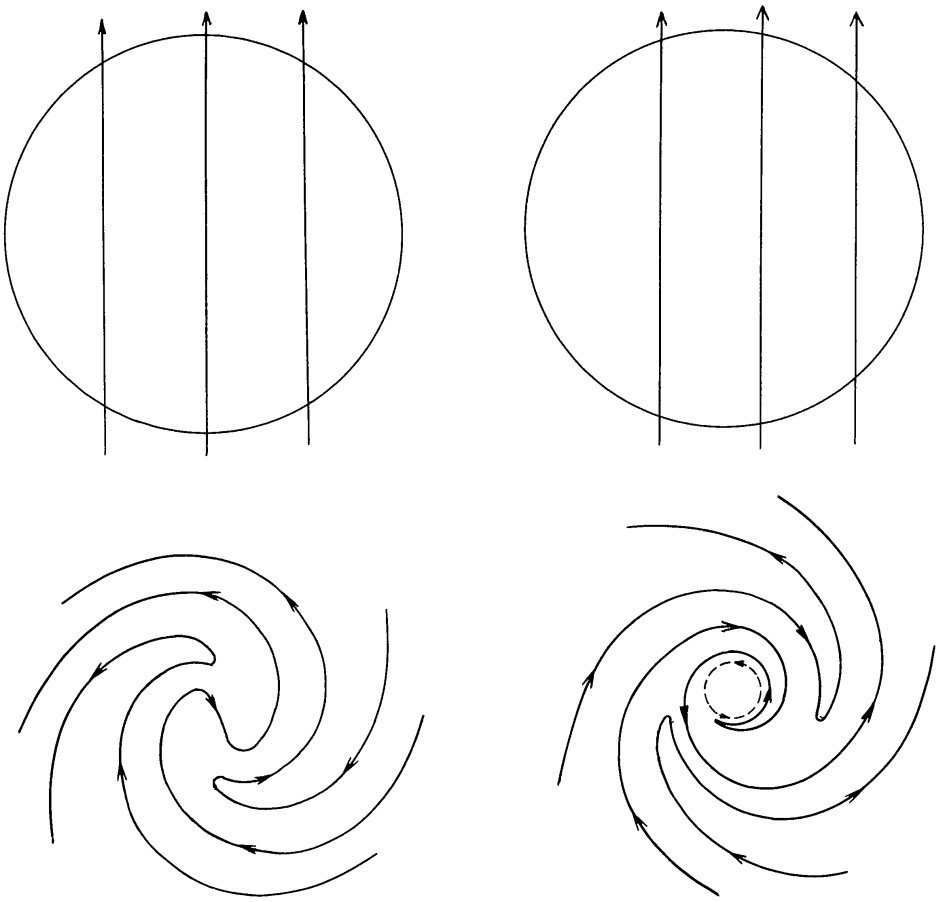

Figure 10 (*a*) Uniform intergalactic magnetic field is twisted by differential rotation to create a BSS field. (*b*) Nonuniform or asymmetric intergalactic magnetic field is twisted to create a circular field in the inner region and a BSS field in the outer region of the disk.

ACKNOWLEDGMENT

This work was done as part of the exchange program between NRO and MPIfR under support by the Japanese Society of Promotion of Sciences. One of us (MF) expresses his thanks to the Ministry of Education of Japan for the scientific research fund under Grant No. 60540156 (1985, 1986).

Literature Cited

Aannestad, P. A., Purcell, E. M. 1973. *Ann. Rev. Astron. Astrophys.* 11: 309
Akasofu, S.-I., Hakamada, K. 1982. *Ap. J.* 253: 552
Allen, R. J., Baldwin, J. E., Sancisi, R. 1978. *Astron. Astrophys.* 62: 397
Appenzeller, I. 1967. *Publ. Astron. Soc. Pac.* 79: 600
Baldwin, J. E. 1959. In *Radio Astronomy*, *IAU Symp. No. 9*, ed. R. N. Bracewell, p. 460. Stanford, Calif: Stanford Univ. Press
Beck, R. 1979. PhD thesis. Univ. Bonn, W. Germ.
Beck, R. 1982. *Astron. Astrophys.* 106: 121

Beck, R. 1983. In *Internal Kinematics and Dynamics of Galaxies, IAU Symp. No. 100*, ed. E. Athanassoula, p. 159. Dordrecht: Reidel
Beck, R., Berkhuijsen, E. M., Wielebinski, R. 1980. *Nature* 283: 272
Beck, R., Biermann, P., Emerson, D. T., Wielebinski, R. 1979. *Astron. Astrophys.* 77: 25
Beck, R., Klein, U., Krause, M. 1985. *Astron. Astrophys.* 152: 237
Begelman, M. C., Blandford, R. D., Rees, M. J. 1984. *Rev. Mod. Phys.* 56(2): 255
Beuermann, K., Kaubach, G., Berkhuijsen, E. 1985. *Astron. Astrophys.* In press
Bingham, R. G., McMillan, R., Pallister, W. S., White, C., Axon, D. J., Scarrott, S. M. 1976. *Nature* 259: 463
Bok, B. J. 1966. *Ann. Rev. Astron. Astrophys.* 4: 95
Bregman, J. N. 1980. *Ap. J.* 236: 577
Bregman, J. N. 1981. *Ap. J.* 250: 7
Buczilowski, U. R. 1985. PhD thesis. Univ. Bonn, W. Germ.
Burn, G. J. 1966. *MNRAS* 133: 67
Chandrasekhar, S. 1961. *Hydrodynamic and Hydromagnetic Stability*. New York: Dover
Chandrasekhar, S., Fermi, E. 1953. *Ap. J.* 118: 113
Cowling, T. G. 1981. *Ann. Rev. Astron. Astrophys.* 19: 115
Davis, L., Greenstein, J. L. 1951. *Ap. J.* 114: 206
de Boer, K. S., Savage, B. D. 1983. *Ap. J.* 265: 210
de Bruyn, A. G. 1977. *Astron. Astrophys.* 58: 221
Deinzer, W. 1976. *Mitt. Astron. Ges.* 40: 156
de Jong, J., Klein, U., Wielebinski, R., Wunderlich, E. 1985. *Astron. Astrophys.* 147: L6
Duric, N., Seaquist, E. R., Crane, P. C., Davis, L. E. 1983. *Ap. J. Lett.* 273: L11
Ekers, R. D., Sancisi, R. 1977. *Astron. Astrophys.* 54: L973
Ellis, R. S., Axon, D. J. 1978. *Astrophys. Space Sci.* 54: 425
Elvius, A. 1969. *Lowell Obs. Bull.* 7: 117
Elvius, A. 1972. *Astron. Astrophys.* 19: 193
Elvius, A. 1978a. *Astrophys. Space Sci.* 55: 49
Elvius, A. 1978b. In *The Structure and Properties of Nearby Galaxies, IAU Symp. No. 77*, ed. E. Berkhuijsen, R. Wielebinski, p. 65. Dordrecht: Reidel
Elvius, A., Hall, J. S. 1964. *Lowell Obs. Bull.* 6: 123
Elvius, A., Herlofson, N. 1960. *Ap. J.* 131: 775
Fujimoto, M. 1966. In *Nonstable Phenomena in Galaxies, IAU Symp. No. 29*, p. 435
Fujimoto, M., Kawabata, K., Sofue, Y. 1971. *Prog. Theor. Phys. Suppl.* 49: 181
Fujimoto, M., Sawa, T. 1981. *Publ. Astron. Soc. Jpn.* 32: 265
Fujimoto, M., Sawa, T. 1986. *Publ. Astron. Soc. Jpn.* Submitted for publication
Fujimoto, M., Tosa, M. 1980. *Publ. Astron. Soc. Jpn.* 32: 567
Gardner, F. F., Whiteoak, J. B. 1966. *Ann. Rev. Astron. Astrophys.* 4: 245
Georgelin, Y. M., Georgelin, Y. P. 1976. *Astron. Astrophys.* 49: 57
Ginzburg, V. L., Syrovatskii, S. I. 1965. *Ann. Rev. Astron. Astrophys.* 3: 297
Ginzburg, V. L., Syrovatskii, S. I. 1969. *Ann. Rev. Astron. Astrophys.* 7: 375
Gioia, M., Gregorini, L., Klein, U. 1982. *Astron. Astrophys.* 116: 164
Gleesen, L. J., Legg, M. P. C., Westfold, K. C. 1974. *MNRAS* 168: 379
Gräve, R., Beck, R. 1986. *Astron. Astrophys.* In press
Habe, A., Ikeuchi, S. 1980. *Prog. Theor. Phys.* 64: 1995
Haynes, R. F., Klein, U., Wielebinski, R., Murray, J. O. 1986. *Astron. Astrophys.* In press
Heiles, C. 1976. *Ann. Rev. Astron. Astrophys.* 14: 1
Helou, G., Soifer, B. T., Rowan-Robinson, M. 1985. *Ap. J. Lett.* 298: L7
Hiltner, W. A. 1956. *Ap. J. Suppl.* 2: 389
Hiltner, W. A. 1958. *Ap. J.* 128: 9
Hoyle, F., Ireland, J. G. 1961. *MNRAS* 122: 35
Hummel, E. 1980. *Astron. Astrophys. Suppl.* 41: 151
Hummel, E. 1981. *Astron. Astrophys.* 93: 93
Hummel, E., Sancisi, R., Ekers, R. D. 1984a. *Astron. Astrophys.* 133: 1
Hummel, E., Smith, P., van der Hulst, J. M. 1984b. *Astron. Astrophys.* 137: 138
Inoue, M., Tabara, H. 1981. *Publ. Astron. Soc. Jpn.* 33: 603
Jura, M. 1979. *Ap. J.* 229: 485
Jura, M. 1982. *Ap. J.* 258: 59
Kaplan, S. A., Pickelner, S. B. 1970. *The Interstellar Medium*, p. 396. Cambridge, Mass: Harvard Univ. Press
King, D. J. 1983. *Mercury* 1983 (March–April): 46
Klein, U. 1982. *Astron. Astrophys.* 116: 175
Klein, U., Beck, R., Buczilowski, U. R., Wielebinski, R. 1982. *Astron. Astrophys.* 108: 176
Klein, U., Emerson, D. T. 1981. *Astron. Astrophys.* 94: 29
Klein, U., Gräve, R., Wielebinski, R. 1983a. *Astron. Astrophys.* 117: 332
Klein, U., Urbanik, M., Beck, R., Wielebinski, R. 1983b. *Astron. Astrophys.* 127: 177
Klein, U., Wielebinski, R., Beck, R. 1984. *Astron. Astrophys.* 133: 19

Krause, M., Beck, R., Klein, U. 1984. *Astron. Astrophys.* 138: 385
Kronberg, P. P., Simard-Normandin, M. 1976. *Nature* 263: 653
Layzer, D., Rosner, R., Doyle, H. T. 1979. *Ap. J.* 229: 1126
Legg, M. P. C., Westfold, K. C. 1968. *Ap. J.* 154: 499
Levy, E. H. 1974. *Ap. J.* 187: 361
Levy, E. H. 1978. In *The Structure and Properties of Nearby Galaxies, IAU Symp. No. 77*, ed. E. M. Berkhuijsen, R. Wielebinski, p. 57. Dordrecht: Reidel
Lin, C. C. 1971. In *Highlights of Astronomy*, ed. C. de Jager, 2: 88–121. Dordrecht: Reidel
Lin, C. C., Shu, F. H. 1964. *Ap. J.* 140: 646
Lin, C. C., Yuan, C., Shu, F. H. 1968. *Ap. J.* 155: 721
Lipunov, V. M. 1979. *Sov. Astron. AJ* 23: 559
Lynds, C. R., Sandage, A. R. 1963. *Ap. J.* 137: 1005
Manchester, R. N. 1974. *Ap. J.* 188: 637
Manchester, R. N., Taylor, J. H. 1977. *Pulsars*, pp. 123–46. San Francisco: Freeman
Martin, P. G., Shawl, S. J. 1979. *Ap. J. Lett.* 231: 57
Martin, P. G., Shawl, S. J. 1982. *Ap. J.* 253: 86
Mathewson, D. S., Ford, V. L. 1970. *Ap. J. Lett.* 160: L43
Mathewson, D. S., Ford, V. L. 1970b. *Mem. R. Astron. Soc.* 74: 139
Mathewson, D. S., van der Kruit, P. C., Brown, W. N. 1972. *Astron. Astrophys.* 17: 468
Mikhailov, A. A., Syrovatskii, S. I. 1980. *Sov. Astron. Lett.* 6: 78
Moffat, H. K. 1970. *J. Fluid Mech.* 44: 705
Moffat, H. K. 1978. *Magnetic Field Generation in Electrically Conducting Fluids*, pp. 145–78. Cambridge: Cambridge Univ. Press
Moffet, A. T. 1973. In *Galaxies and the Universe*, ed. A. Sandage, M. Sandage, J. Kristian, Vol. 9, Chap. 7. Chicago: Univ. Chicago Press
Morris, D., Berge, G. L. 1964. *Ap. J.* 139: 1388
Ohki, T., Fujimoto, M., Hitotuyanagi, Z. 1964. *Prog. Theor. Phys. Suppl.* 31: 77
Öhman, Y. 1942. *Stockholm Obs. Ann.* 14(4): 1
Ondrechen, M. P. 1985. *Astron. J.* 90: 1474
Pacholczyk, A. G. 1963. *Acta Astron.* 14: 1
Pacholczyk, A. G. 1976. In *Lecture Notes on Introductory Theoretical Astrophysics*, ed. R. J. Weymann et al., pp. 151–93. Tucson: Pachart
Parker, E. N. 1970. *Ap. J.* 162: 665
Parker, E. N. 1971a. *Ap. J.* 163: 255
Parker, E. N. 1971b. *Ap. J.* 166: 295
Parker, E. N. 1975. *Ann. NY Acad. Sci.* 257: 141
Parker, E. N. 1979. *Cosmical Magnetic Fields*, pp. 795–819. Oxford: Clarendon
Phillips, S., Kearsey, S., Osborne, J. L., Haslam, C. G. T., Stoffel, H. 1981. *Astron. Astrophys.* 103: 405
Piddington, J. H. 1964. *MNRAS* 128: 345
Piddington, J. H. 1969. *Cosmic Electrodynamics*, pp. 245–69. New York: Wiley-Interscience
Piddington, J. H. 1972. *Cosmic Electrodyn.* 3: 129
Piddington, J. H. 1978. *Astrophys. Space Sci.* 59: 237
Piddington, J. H. 1981. *Astrophys. Space Sci.* 80: 457
Pismis, P. 1960. *Bol. Obs. Tonantzintla Tachubaya.* 2: 3
Pismis, P. 1984. *Astrophysica* 20: 7
Pooley, G. G. 1969. *MNRAS* 144: 101
Purcell, E. M., Spitzer, L. 1971. *Ap. J.* 167: 31
Roberts, W. W. 1969. *Ap. J.* 158: 123
Roberts, W. W. 1975. *Vistas Astron.* 19: 91
Roberts, W. W., Hantley, J. M., van Albada, G. D. 1979. *Ap. J.* 233: 67
Roberts, W. W., Yuan, C. 1970. *Ap. J.* 161: 877
Ruzmaikin, A. A., Shukurov, A. M. 1981. *Sov. Astron. AJ* 25: 533
Ruzmaikin, A. A., Sokolov, D. D., Shukurov, A. M. 1985. *Astron. Astrophys.* 148: 335
Ruzmaikin, A. A., Sokolov, D. D., Turchaminov, V. I. 1980. *Sov. Astron. AJ* 24: 182
Sandage, A. R. 1961. *The Hubble Atlas of Galaxies*, pp. 26, 36. Washington, DC: Carnegie Inst. Washington
Sanders, R. H., Huntley, J. M. 1976. *Ap. J.* 209: 53
Sanders, R. H., Tubbs, A. D. 1980. *Ap. J.* 235: 803
Savage, B. D., de Boer, K. S. 1979. *Ap. J. Lett.* 230: L7
Savage, B. D., de Boer, K. S. 1981. *Ap. J. Lett.* 243: 460
Savage, B. D., Mathis, J. S. 1979. *Ann. Rev. Astron. Astrophys.* 17: 73
Sawa, T., Fujimoto, M. 1980. *Publ. Astron. Soc. Jpn.* 32: 551
Sawa, T., Fujimoto, M. 1986. *Publ. Astron. Soc. Jpn.* 38: 133
Scarrott, S. M., White, C., Pallister, W. S., Solinger, A. B. 1977. *Nature* 265: 32
Schmidt, G. D., Angel, J. R. P., Cromwell, R. H. 1976. *Ap. J.* 206: 888
Schmidt, Th. 1970. *Astron. Astrophys.* 6: 294
Schmidt, Th. 1976. *Astron. Astrophys. Suppl.* 34: 357
Schüssler, M. 1979. *Astron. Astrophys.* 72: 348

Scoville, N. Z., Soifer, B. T., Neugebauer, G., Young, J. S., Matthews, K., Yerka, J. 1985. *Ap. J.* 289: 129
Segalovitz, A. 1976. PhD thesis. Univ. Leiden, Neth.
Segalovitz, A., Shane, W. W., de Bruyn, A. G. 1976. *Nature* 264: 272
Simard-Normandin, M., Kronberg, P. P. 1979. *Nature* 279: 115
Simard-Normandin, M., Kronberg, P. P. 1980. *Ap. J.* 242: 74
Sofue, Y., Fujimoto, M. 1983. *Ap. J.* 265: 722
Sofue, Y., Fujimoto, M., Kawabata, K. 1979. *Publ. Astron. Soc. Jpn.* 31: 125
Sofue, Y., Klein, U., Beck, R., Wielebinski, R. 1985. *Astron. Astrophys.* 144: 257
Sofue, Y., Takano, T. 1981. *Publ. Astron. Soc. Jpn.* 33: 47
Sofue, Y., Takano, T., Fujimoto, M. 1980. *Astron. Astrophys.* 91: 335
Sofue, Y., Tosa, M. 1974. *Astron. Astrophys.* 36: 237
Solinger, A. B. 1967. *Astron. J.* 72: 830
Solinger, A. B., Markert, T. 1975. *Ap. J.* 197: 309
Solomon, P. M. 1983. In *Internal Kinematics and Dynamics of Galaxies, IAU Symp. No. 100*, ed. E. Athanassoula, p. 35. Dordrecht: Reidel
Sorensen, S. A., Matsuda, T., Fujimoto, M. 1976. *Astrophys. Space Sci.* 43: 491
Soward, A. M. 1978. *Astron. Nachr.* 299: 25
Spitzer, L. Jr. 1956. *Ap. J.* 124: 20
Spitzer, L. Jr. 1978. *Physical Processes in the Interstellar Medium*, pp. 149–70. New York: Wiley-Interscience
Spoelstra, T. A. Th. 1977. *Sov. Phys. Usp.* 20: 336
Stix, M. 1975. *Astron. Astrophys.* 42: 85
Stix, M. 1976. *Astron. Astrophys.* 47: 243
Tabara, H., Inoue, M. 1980. *Astron. Astrophys. Suppl.* 39: 379
Thomson, R. C., Nelson, A. H. 1980. *MNRAS* 191: 863
Tosa, M. 1973. *Publ. Astron. Soc. Jpn.* 25: 191
Tosa, M., Fujimoto, M. 1978. *Publ. Astron. Soc. Jpn.* 30: 315
Tosa, M., Sofue, Y. 1974. *Astron. Astrophys.* 32: 461
Vainshtein, A. A., Ruzmaikin, A. A. 1971. *Sov. Astron. AJ* 15: 714
Vallée, J. P. 1982. *Ap. J. Lett.* 261: L55
Vallée, J. P. 1983a. *Astron. Astrophys.* 23: 85
Vallée, J. P. 1983b. *Astron. Astrophys.* 124: 147
Vallée, J. P. 1984. *J. R. Astron. Soc. Can.* 78: 57
van Albada, G. D. 1978. PhD thesis. Univ. Leiden, Neth.
van Albada, G. D., van der Hulst, J. M. 1982. *Astron. Astrophys.* 115: 263
van der Kruit, P. C. 1973. *Astron. Astrophys.* 29: 263
van der Kruit, P. C., Allen, R. J. 1976. *Ann. Rev. Astron. Astrophys.* 14: 417
van der Kruit, P. C., Oort, J. H., Mathewson, D. S. 1972. *Astron. Astrophys.* 21: 169
Verschuur, G. L. 1974. In *Galactic and Extragalactic Radio Astronomy*, ed. G. L. Verschuur, K. I. Kellermann, p. 179. Berlin: Springer-Verlag
Verschuur, G. L. 1979. *Fundam. Cosmic Phys.* 5: 113
Visvananthan, N. 1974. *Ap. J.* 191: 319
Webster, A. 1975. *MNRAS* 171: 243
Webster, A. 1978. *MNRAS* 185: 507
Weller, G. L., Perry, J. J., Kronberg, P. P. 1984. *Ap. J.* 279: 19
Wentzel, D. G. 1960. *Bull. Astron. Soc. Neth.* 498: 103
Werner, W. 1985. *Astron. Astrophys.* 144: 502
White, M. P. 1978. *Astron. Nachr.* 299: 209
Wielebinski, R. 1983. *Proc. Int. Conf. Cosmic Rays, 18th, Bangalore*, 2: 161–64
Wielebinski, R. 1985. *Rev. Mex. Astron. Astrofis.* 10: 69
Wielebinski, R., von Kap-herr, A. 1977. *Astron. Astrophys.* 59: L17
Wunderlich, E. 1985. MSc thesis. Univ. Bonn, W. Germ.
York, D. G. 1982. *Ann. Rev. Astron. Astrophys.* 20: 221
Zeldovich, Ya. B., Ruzmaikin, A. A., Sokolov, D. D. 1983. *Magnetic Fields in Astrophysics, Fluid Mech. Astrophys. Geophys.*, Vol. 3. New York: Gordon & Breach